April 2014

The effect of flavonoids on artemisinin transport across Caco-2 monolayers

Brianna Susan Hayes
Worcester Polytechnic Institute

Kate Lebzelter Harten
Worcester Polytechnic Institute

Laura Marie Burns
Worcester Polytechnic Institute

The effect of flavonoids on artemisinin transport across Caco-2 monolayers

A Major Qualifying Project Proposal

Submitted to the faculty of

Worcester Polytechnic Institute

In partial fulfillment of the requirements for the

Degree of Bachelor of Science

(PZW - AAF5)

By

Kate Harten, Brianna Hayes, Laura Sandford

April 30, 2014

Dr. Pamela J. Weathers, MQP Advisor

Abstract

Malaria is currently treated with artemisinin (AN), a drug extracted from the plant *Artemisia annua* L.. Although many AN based combination therapies (ACTs) have long been effective in treating malaria, recent studies have suggested that the orally delivered dried leaves of the whole plant (pACT) also contain flavonoids that work synergistically with AN. Thus, pACT has recently been proposed as an effective and more affordable alternative for malaria treatment.

In this study, this treatment was investigated by examining the effect of flavonoids on AN bioavailability. This was studied by examining the transport of AN alone and in conjunction with quercetin (Q) or rutin (R) across Caco-2 cell monolayers grown on 12-well permeable cell culture inserts. The Caco-2 cell monolayers were used to simulate the intestinal epithelium, thus providing a model for drug transport within the human body. To ensure that the monolayers were confluent enough to use in drug transport experiments and that they would not be damaged by the ethanol present in the apical solutions, representative monolayers were tested under controlled conditions using a Lucifer Yellow (LY) assay. The LY assays resulted in percent LY rejection values of greater than 75%, so the remaining monolayers were deemed confluent enough for the drug transport experiments.

To determine the baseline for AN transport alone, apical to basolateral transport of AN was measured. To determine whether or not Q and R increased the transport rate or amount of AN across the monolayer, equimolar amounts of each flavonoid, in addition to AN, were added to the apical side of transwell inserts. The basolateral volumes were sampled every 15 minutes for one hour, extracted with methylene chloride and dried under N_2 gas. AN was analyzed in the extracts by GC/MS and transport rates calculated ± Q and ± R. This study demonstrated that, although both Q and R increased the rate of AN transport, only R increased the rate significantly. These findings may lead to a better understanding of the function of flavonoids in pACT.

Acknowledgements

Our team would like to express our sincere gratitude to the following individuals for supporting us throughout the completion of this project. We are incredibly grateful for our advisor, Dr. Pamela Weathers, for guiding, assisting, and sponsoring us throughout the completion of this project. She has provided us with an extraordinary opportunity to develop our skills as professional biologists and to collaborate with her knowledgeable lab team, which will impact all of our future work in a wonderful way. We would like to thank Dr. Melissa Towler, who is a part of that fantastic lab team, for providing us with invaluable technical expertise and conducting all of the GC/MS analysis for our project. We would also like to thank the other laboratory team members: Ying Yang, Liwen Fei, Sibo Wang, Hailey Cambra, Jason Purnell, and Meredith Ghilardi, for actively listening to our project presentations and offering helpful feedback and recommendations about our experimental designs. Finally, we would like to thank Dr. Jill Rulfs, Associate Professor of Biology and Biotechnology, for training us to be effective in the cell culture laboratory and advising our laboratory work. Our project could not have succeeded without any of these people, who have all contributed their time and effort to improve our project.

Table of Contents

1.0 Introduction

Half of the world's population is currently at risk of contracting malaria (WHO, 2013). Although malaria is a curable disease, most of the people who suffer from malaria do not have the resources to protect themselves from mosquitoes or obtain affordable health care. Because of the socioeconomic status of those at risk for malaria, the death toll is high. In 2010, an estimated 655,000 people died of malaria (WHO, 2013).

In spite of the global malaria eradication efforts that were undertaken by the World Health Organization (WHO) in the last century, many impoverished people in South America, Asia, and Africa still suffer from the ubiquitous transmission of malaria (CDC, 2012). Malaria endemic-societies are affected not only medically and emotionally by the disease, but are also impacted on a socioeconomic level. In 2012, the Centers for Disease Control and Prevention (CDC) estimated that at least 12 billion US dollars per year were spent worldwide on illness, treatment, and premature death due to malaria (CDC, 2012). Malaria therefore contributes to the cycle of poverty by depressing economic development, which in turn results in the delayed development of the necessary infrastructure for accessible healthcare.

The WHO is currently using multiple approaches to address the malaria epidemic. Preventive interventions such as the use of insecticides and bed nets have been somewhat successful. However, once a person is infected, immediate treatment with antimalarial drugs offers the best chance at helping that person. Today, the WHO recommends a treatment called Artemisinin Combination Therapy (ACT) as the first-line drug treatment for uncomplicated *P. falciparum* malaria (WHO, 2013). ACT is highly effective, and it works by using AN, produced by the plant *Artemisia annua*, in combination with a partner drug to prevent AN drug resistance from emerging. However, for many of the people who suffer from malaria, ACT is unaffordable and inaccessible (Mutabingwa, 2005).

Recent research about the possibility of an *A. annua* whole plant treatment (pACT) suggests that it may be a more effective and sustainable treatment for malaria than ACT (Weathers et al., 2010; Elfawal et al., 2012). Mouse studies showed that the dried plant delivers a larger amount of AN to the bloodstream than the pure drug (Weathers et al., 2010; Weathers et al., 2014a). Although the reason for this has not been determined, it is hypothesized that the increased bioavailability may be due to the other compounds, such as flavonoids, present in the

plant. Plant maturation and delivery methods can impact the amount of AN and flavonoids available in *A. annua*. In particular, AN increases as leaves mature. AN also increases during the process of drying and tableting for oral administration of pACT (Weathers and Towler 2014, unpublished). Such compounds could enhance the transport of AN across the intestinal cell epithelium. Additionally, although pACT is still being investigated, it has the potential to overcome some of the difficulties associated with the current antimalarial treatment options, such as affordability, accessibility, and drug resistance.

In order to test the hypothesis that flavonoids present in the plant enhance the transport of AN, thereby increasing bioavailability of AN on the basolateral, or serosal, side of the monolayer, this project used a Caco-2 monolayer to study drug transport across the intestinal epithelium. Enhanced bioavailability was demonstrated, which further supports the argument that pACT is a more effective treatment for malaria than the currently established, but unaffordable, treatment options.

2.0 Literature Review

2.1 Malaria

Malaria is a highly infectious, mosquito-borne disease that is prevalent in South America, Asia, and Africa. The tropical and subtropical environments that are found on these continents are the perfect breeding ground for the *Anopheles* mosquito, which is capable of transmitting malaria to a human from a single bite (Barry, 2010). Malaria is most common in low-income developing countries, where people do not have the resources to protect themselves from mosquitoes (WHO, 2012). Although the number of deaths attributed to malaria has decreased from 2002 to 2012 due to drug treatments (such as ACT), vector control, insecticides, and the distribution of mosquito nets, > 500,000 deaths still occur each year (WHO, 2012).

2.1.1 Biology

Malaria is a blood disease caused by five different parasite species—*Plasmodium falciparum, P. vivax, P. ovale, P. malariae, and P. knowlesi.* The life cycle of the malaria parasite begins in a human when an infected mosquito transmits malaria sporozoites through a bite (Fig. 1; Lawrence Berkley Laboratory, 2001).

The sporozoites then travel to and subsequently enter liver cells, and multiply thousands of times before bursting from the liver and entering the red blood cells in the blood stream. Within the first 48 hours of infecting a red blood cell, the malaria parasite undergoes several stages of development. In the first stage, "ring stage," the parasite begins to ingest the contents of the infected cell (Barry, 2010). The next developmental stage is the trophozoite stage, during which the parasite continues metabolizing hemoglobin, grows larger, and prepares to reproduce. In the final stage, the parasite divides to form a multinucleated schizont. At the end of this cycle, the red blood cell ruptures and the parasites are disseminated to infect more red blood cells (Lawrence Berkley Laboratory, 2001; Fig. 1).

Of all the strains, *P. falciparum* most often causes critical and life-threatening malaria (CDC, 2013). *P. falciparum* multiplies extremely rapidly in the blood and changes the adhesive properties of the red blood cells it inhabits. This change causes the red blood cells to stick to the walls of blood vessels resulting in severe blood loss and anemia (Lawrence Berkley Laboratory, 2001;CDC, 2012).

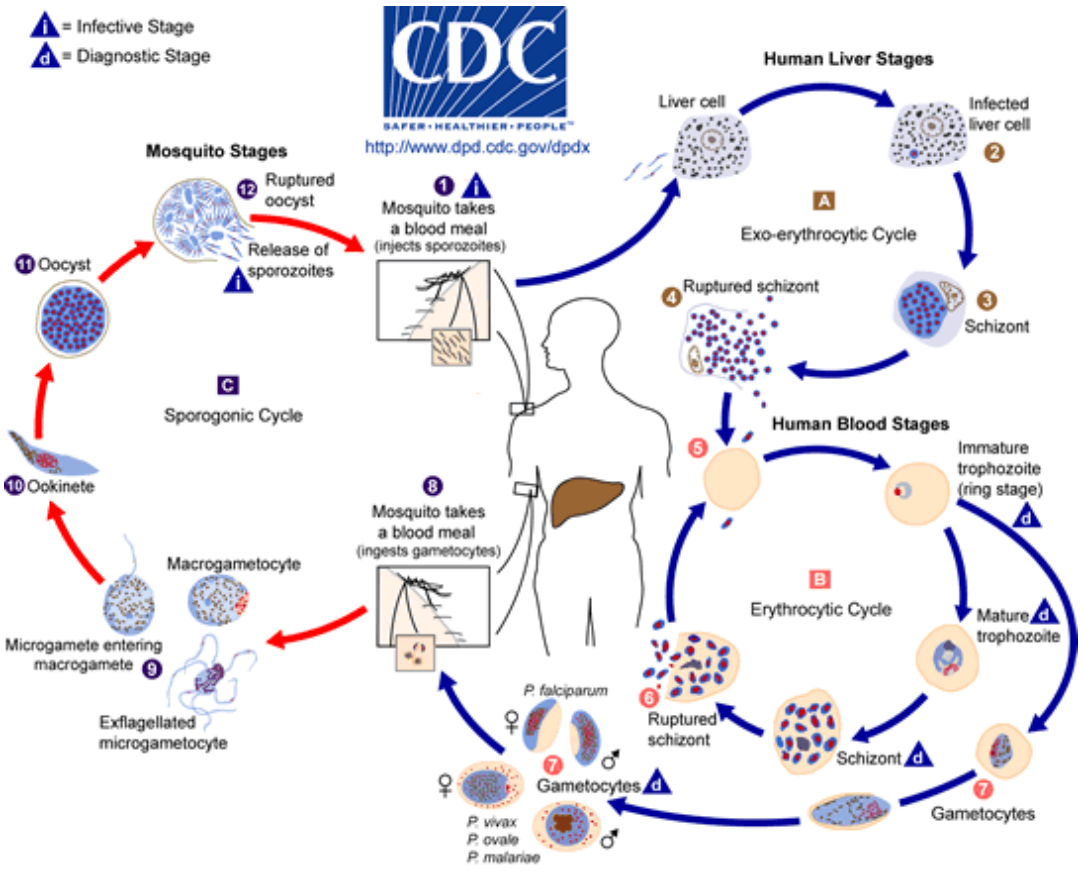

Figure 1: Life cycle of malaria parasite (CDC, 2012)

Although *P. falciparum* is the most dangerous, all strains have their own risks. For example, *P. vivax* and *P. ovale* have dormant liver stages that can activate suddenly and invade the blood, effectively causing the human host to relapse, several months or years after the infecting mosquito bite (CDC, 2012). Additionally, *P. malariae* causes a long-lasting, chronic infection that in some cases can last a lifetime if it is untreated.

2.1.2 Signs and Symptoms

The symptoms caused by the five strains of malaria are similar. In most patients, the first symptoms will be felt 10 days to 4 weeks after infection. The initial symptoms are flu-like; fever, chills, headaches, muscle aches, and fatigue are common. However, if the disease is untreated, the symptoms may become more serious, including vomiting, diarrhea, anemia, jaundice, kidney failure, seizures, mental confusion, coma, and death (CDC, 2012). Because the symptoms can become so severe, it is imperative that patients with malaria seek immediate treatment. However, the availability of medical care depends on the geographical location and socioeconomic status of the patient in question.

2.1.3 Demographics

Several factors, such as age, gender, geographical location, socioeconomic status, regional government, and availability of health care, determine whether or not a person contracts malaria. The two primary determining factors for risk of malaria transmission that will be the focus of this paper are geographical location and socioeconomic status, because these factors are arguably the largest determining factors of malaria risk. For example, the 2010 World Malaria Report stated that in 2010, of the 655,000 estimated deaths, the majority of which were children, 91% were in Africa (WHO, 2010). This illustrates the importance of geographical location. Prior studies also highlighted the importance of socioeconomic status as a risk factor for malaria (Sachs & Malaney, 2002; Stratton et al., 2008).

2.1.3.1 Geographical Location

Climatic factors such as temperature, humidity, and rainfall often determine where malaria transmission occurs in the world (Hay et al., 2004). These factors must be ideal for the *Anopheles* mosquito to survive and reproduce, and for the parasite to complete its growth in *Anopheles* before it can be transmitted. At temperatures below 20°C, *P. falciparum* cannot complete its growth cycle in the mosquito, and thus cannot be transmitted to human hosts (CDC, 2012). Because of this temperature constraint, *P. falciparum* is very common in many countries in Africa south of the Sahara desert. Of the human population at risk of contracting malaria via *P. falciparum* infection, 75% live in ten countries: India, China, Indonesia, Bangladesh, Pakistan, Nigeria, Vietnam, Thailand, Democratic Republic of the Congo and the Philippines (Guerra et al., 2006).

Malaria is commonly transmitted in the tropical and subtropical areas of Africa, Asia, and South America (Figure 2), where the climatic factors are ideal for the survival of the *Anopheles* mosquito and the transmission of the malaria parasites into human hosts (CDC, 2012). Due to a cooler climate, economic development, and successful public health initiatives, citizens of Western Europe and the United States do not commonly suffer from malaria. The presence of the *Anopheles* mosquito in these countries, however, as well as global warming, indicate that citizens are at a constant risk of the disease being reintroduced into these areas (CDC, 2012).

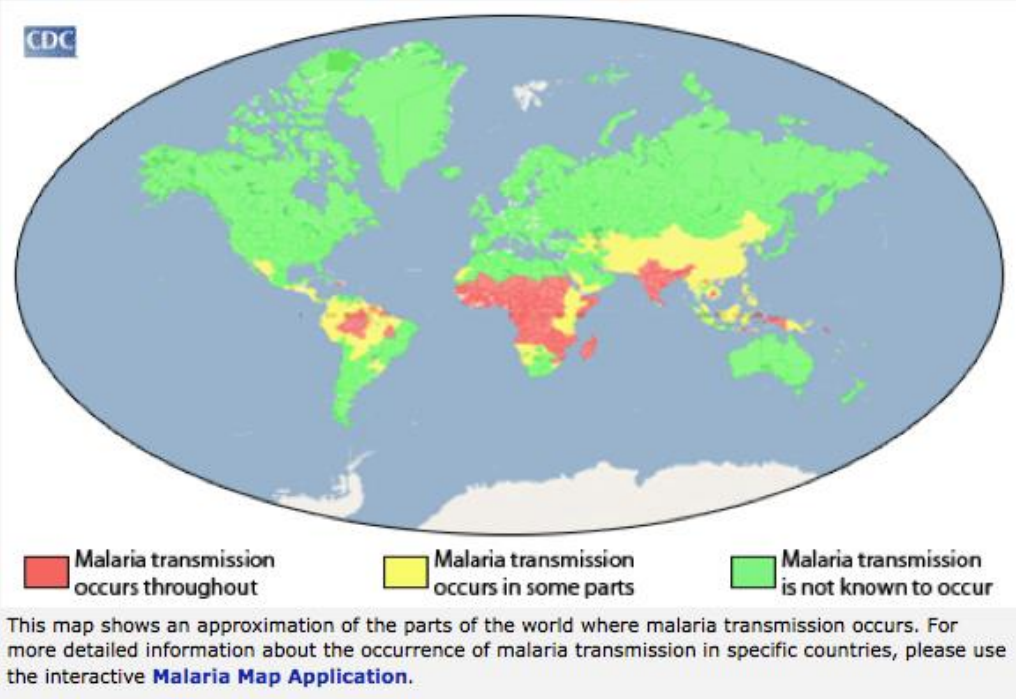

Figure 2: A world map showing the prevalence of malaria transmission by geographical region (CDC, 2012).

2.1.3.2 Socioeconomic Status

Malaria is prevalent in some of the poorest areas of the world, and the costs associated with ubiquitous malaria transmission further depress economic development, which leads to an inability to pay for healthcare or preventative measures for malaria (such as insecticides or bed nets). The constant transmission of malaria in endemic African countries diminished annual economic growth by >1% per person from 1965 to 1990 (Sachs & Malaney, 2002).

In 2012, the Centers for Disease Control and Prevention (CDC) estimated the direct costs of malaria for the world and that at least 12 billion USD per year were spent worldwide on illness, treatment, and premature death due to malaria. The CDC also stated, "costs are many times more than that in lost economic growth," (CDC, 2012). Therefore, malaria contributes to the cycle of poverty in poor and underdeveloped areas.

2.1.4 Eradication Efforts

In the past, many efforts were made to eradicate malaria. Insecticides, political and social mobilization efforts, and environmental modifications (such as destroying the habitat of the *Anopheles* mosquito or distributing bed nets) were used (CDC, 2012). However, all of those efforts were preventive interventions, and did not help those already suffering from the disease.

Because malaria can be severe, immediate treatment of infected patients with antimalarial drugs offers the best chance at helping those patients and their surrounding community.

The successful use of drugs and preventive interventions, including the widespread use of DDT, resulted in the eradication of malaria in the United States and Western Europe in the mid-1900s (Harrison, 1978). This was likely because these areas have cooler climates and more developed infrastructures than the areas currently plagued by malaria. Despite success in the United States and Europe, worldwide eradication of malaria largely failed. Malaria continues to be a major health issue for many people in Africa, Asia, and South America today. In fact, more people are killed by malaria currently than 40 years ago (Stratton et al., 2008). This indicates that new strategies are needed to control the transmission of the disease.

2.2 Artemisinin

In the 1970's, scientists noticed that protozoans of the genus *Plasmodium* were gaining resistance to the anti-malarial drugs that were on the market. Research into a new treatment with the herb *Artemisia annua* L. began. *A. annua* prepared as a tea infusion was used as a remedy for fevers in China for >2,000 years (Kew Royal Botanical Gardens, 2013). In 1972, it was found that the plant contained a metabolite that exhibited antimalarial properties. This compound was identified as AN (Tu, 2011; Fig. 3)

2.2.1 Classification of Artemisinin

There are two kinds of plant metabolites, primary and secondary. Primary metabolites play a role in the basic life function of plants. They are used in processes like respiration, growth, cell division and reproduction. Secondary metabolites serve many purposes including pigmentation, ultraviolet protection and defense. (Bourgard et al., 2001) The three major groups of secondary metabolites are: phenolics, nitrogenous compounds and terpenes. (Taiz and Zeiger, 2010). Certain secondary metabolites have antibiotic, antiviral and antifungal properties. AN is a secondary plant metabolite with antimicrobial properties.

AN's chemical structure (Figure 3) is classified as a sesquiterpene lactone endoperoxide (Brisibe, 2008). Terpenes are naturally made compounds with a ratio of five carbons to eight hydrogens, they are given a prefix based on the number of 5-C isoprene units contained in the compound. The first part of AN's structural name, "sesquiterpene," refers to a terpene with 15 carbons, 3 isoprene units.

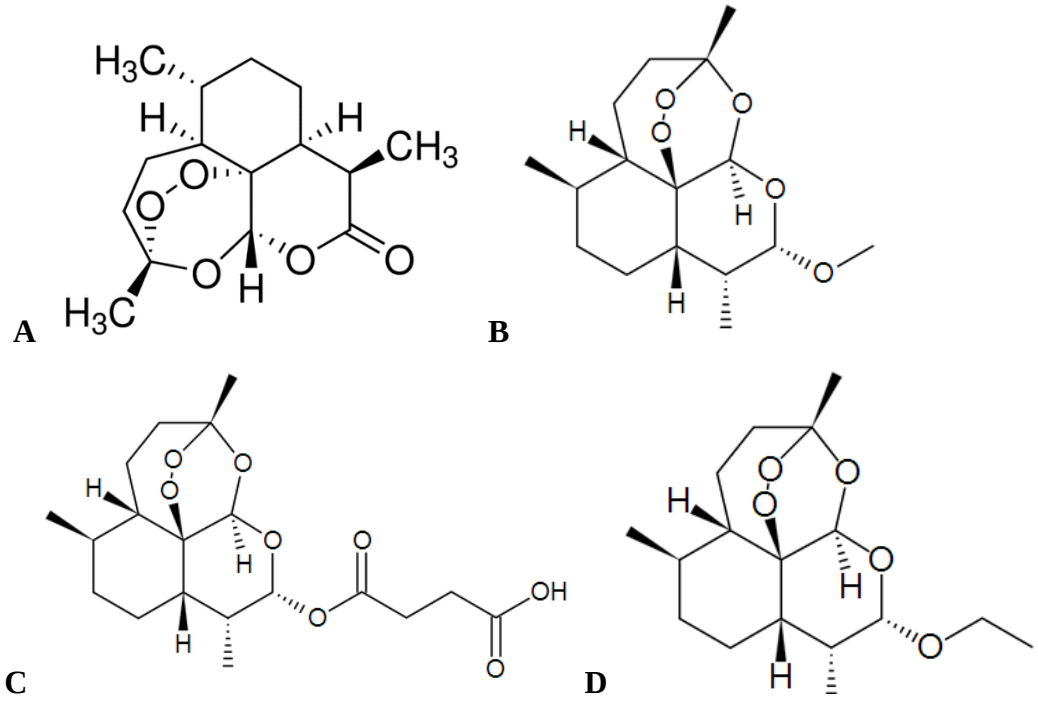

Figure 3: Structure of artemisinin (A), artemether (B), artesunate (C) and artemotil (D) (Wikimedia, 2011a, 2007a, 2007b, 2007c)

The second word describing AN's structure, "lactone" refers to a cyclic compound containing a carbonyl and an ether group. An endoperoxide is a compound containing a single bond between two oxygens located within a ring (Wade, 2010). In AN, the endoperoxide is believed to be responsible for the mechanism of action that causes the compound to be antimalarial (Meshnick, 2002).

2.2.2 Glandular Trichomes

AN is synthesized, secreted and stored by glandular trichomes on the leaves of *A. annua*. Glandular trichomes are protrusions that grow on specialized epidermal cells located on the leaves or other organs of a plant. The number of glandular trichomes on the surface of *A. annua* leaves increases from the third month to the flowering stage of plant development (Guo et al., 2012). Once the plant reaches flowering, the density of glandular trichomes stops increasing. This is why dried leaves used for malaria treatment are harvested just before flowering (Guo et al., 2012). Other compounds secreted by the glandular trichomes include essential oils, phenolics, flavonoids and terpenoids (Wu et al., 2012).

The importance of AN as an antimalarial drug has led to studies of these trichomes. On average AN only makes up 0.01 – 1.1% of the dry weight of *A. annua* (Guo et al., 2012);

increasing this percentage would allow the drug to be more widely used. Efforts in this direction include the identification of intermediate compounds engaged in AN production and the cloning of enzymes involved in the AN biosynthesis pathway (Guo et al., 2012).

2.2.3 Artemisinins and ACTs as Treatment for Malaria

Artemisinins are chemically modified versions of AN extracted from the plant, *Artemisia annua* L. (CDC, 2012). Artesunate is one such AN derivative (Figure 3). In 2007, the Food and Drug Administration (FDA) approved an investigational new drug protocol called "Intravenous Artesunate for Treatment of Severe Malaria in the United States." This allowed artemisinins to be available as an antimalarial treatment in the United States for the first time (CDC, 2012). Currently, artesunate can be obtained from the CDC for use in treating severe malaria with either an inability to take oral medications or an inability to quickly and safely take intravenous quinidine (CDC, 2012).

Artemisinin-based combination therapies (ACTs) combine an AN derivative with a partner drug (Rosenthal, 2008). ACT contains at least two antimalarials within one pill. One of these antimalarials is AN-based, meaning that it is a derivative of AN. The three AN derivatives are: artesunate, artemether and artemotil (Figure 3). Currently, these derivatives may be combined with lumefantrine, amodiqine, mefloquine, sulfadoxine-pyrimethamine, piperaquine or pyronaridine tetraphosphate within an antimalarial pill (World Health Organization, 2012). For example, the drug Coartem® is a combination of the AN deriviative artemether and the synthetic drug lumefantrine (CDC, 2012). This provides a more effective treatment than treating malaria with pure AN, because some species of the *Plasmodium* parasite may have evolved AN-resistance (WHO, 2013). Thus, the use of ACTs is purported to prevent or slow the evolution of AN drug resistance (Bloland, 2001). ACT works by using the AN compound to reduce the main parasite load during the first three days of treatment, while the partner drug eliminates the remaining parasites that may survive due to AN resistance. Because of their efficacy, ACTs are recommended by the WHO as the first-line drug treatment for uncomplicated *P. falciparum* malaria (WHO, 2013).

2.2.4 An Alternative Artemisinin Combination Therapy

Recent research by Elfawal et al. (2012) using *P. chabaudi*-infected mice suggested that orally administered dried leaves of *A. annua* may be more effective at curing the disease than

purified AN. This whole plant treatment is referred to as plant Artemisinin Combination Therapy (pACT). Using the rodent malaria model, *Plasmodium chabaudi*, infected mice were administered a single dose (24 mg AN/kg mouse body weight) of whole plant *A. annua*, a single dose of pure AN (24 mg AN/kg mouse body weight) or a placebo (mouse chow without drug). Mice treated with low-dose whole plant had significantly lower parasitemia than the pure AN treated mice up to 72 hours post treatment. (Elfawal et al., 2012).

In another study conducted by Weathers et al. (2010), the bioavailability, or the rate at which a substance enters the bloodstream, of pure AN was compared to the bioavailability of pACT. When pACT containing 30.7 µg of AN was administered to the mice, a concentration of 0.087 mg L^{-1} was found after only thirty minutes. When pure AN containing 30.7 µg was administered, the drug remained undetectable in the bloodstream 60 minutes after consumption. Eventually, after administering 1,400 µg of pure AN to the mice, the blood concentration reached 0.074 mg L^{-1}. These results suggested that the AN contained in *A. annua* was 45-fold more bioavailable than pure AN. A more recent pharmacokinetic study by Weathers et al. (2014a) showed that the presence of plant material was crucial for movement of large amounts of ANinto the serum.

Few studies have been done on the effect of pACT in humans. Mueller et al. (2000) treated *P. falciparum* infected adults with *A. annua* tea. Despite some success at the beginning of the therapeutic tea trials, after a short period of parasitic inactivity, the *P. falciparum* reemerged (Mueller et al., 2004). These trials suggest that *A. annua* tea, as a therapeutic for malaria, is not a viable option. This is partially due to the difficulty controlling the AN dose in the tea (Weathers et al., 2014c). Another study conducted by the International Centre of Insect Physiology and Ecology (ICIPE) and Kenya Medical Research Institute (KEMRI) showed that 80-91% of the 48 patients treated with varying doses of AN in the form of tableted *A. annua* plant material did not exhibit recrudescence (ICIPE, 2005). A similar study in Bangui, Central Africa found that administration of whole plant therapy capsules containing 0.4-0.5 mg of AN reduced parasitemia by 62% in a group of 25 patients, 22 of whom were children (Onimus et al., 2013). These studies indicated that *A. annua* has the possibility of being an effective AN combination therapy. However more studies of how other compounds in *A. annua* affect AN content are necessary.

2.2.5 Compounds to Investigate

Flavonoids contain aromatic hydrocarbons bonded to a hydroxyl group. Flavonoids are often the pigments in flowers that act as attractants for pollinators, and in fruit for seed dispersal. Flavonoids have antioxidant activity, because they are capable of reacting with and detoxifying free radicals (Pietta, 2000). Many are also antimalarial. In a study by Lehane and Saliba (2008), eleven flavonoids were tested for antiplasmodial activity. Each of the eleven flavonoids showed activity against a chloroquine-resistant strain of *P. falciparum* with IC_{50} values between 12 and 76 µm. Liu et al. (1992) also demonstrated that flavonoids have anti-plasmodial activity. A chloroform extract of *A. annua* cells, in which no artemisinin was detected, was found to have an IC_{50} of 14.5µg/mL. The extract contained methoxylated flavonoids including artemetin, chrysoplenetin, chrysoplenol-D and cirsilineol (Liu et al., 1992). Casticin was not detected in the chloroform extract; however, Elford et al. (1987) showed that casticin in combination with artemisinin assisted in the inhibition of *P. falciparum* growth. Artemetin was less effective in combination with artemisinin but still showed a synergistic effect. This effect was only demonstrated when the flavonoids were combined with artemisinin and did not appear when combined with another anti-malarial, chloroquine. Table 1 shows the IC_{50} values of flavonoids found in *A. annua*.

Table 1: Flavonoids in *A. annua* and their IC_{50} values against *P. falciparum*

Flavonoids	IC_{50} Values (uM)	Reference
Artemetin	26	Liu et al. (1992)
Casticin	24	Elford et al. (1987)
Chrysoplenetin	23	Liu et al. (1992)
Chrysoplenol-D	32	
Cirsilineol	36	
Kaemferol	25 ± 2	Lehane & Saliba (2008)
Luteolin	12 ± 1	
Myrectin	76 ± 23	
Quercetin	14 ± 1	
Rutin	7 ± 10	Ganesh et al. (2012)

It may be that in *A. annua* the flavonoids and AN work in harmony to destroy the parasite, which may explain why pACT is effective (Kim et al., 2007).

For this project, the flavonoids quercetin (Q) and rutin (R) will be studied (Figure 4); R is the glycoside of Q, containing the two rutinose sugars, rhamnose and glucose. R is water soluble and converted into Q when it enters the blood stream (Erlund et al., 2000). Both R and Q are polyphenolic compounds that are found in fruits, vegetables, leaves, herbs, seeds, red wine, coffee, beer and tea (Azevedo et al., 2013).

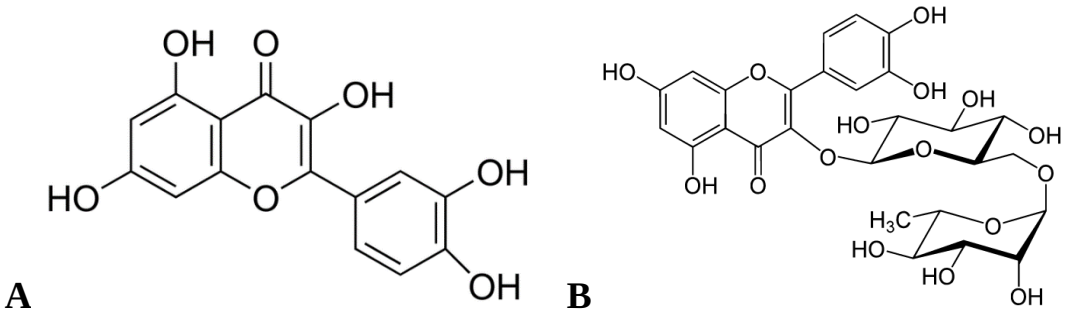

Figure 4: Structure of quercetin (A) and rutin (B) (Wikimedia, 2013, 2009)

In a study by Ganesh et al. (2012), both R and Q inhibited field isolated and lab-adapted *P. falciparum*. R had an IC_{50} that was about half that of Q for the field isolates, showing that R had a greater inhibitory effect on the parasite (Table 1). For one of the two lab-adapted clones of *P. falciparum*, R and Q had IC_{50} values that were statistically the same. For the second lab-adapted clone, R had a higher IC_{50}. This showed that even though both R and Q have anti-plasmodial activity, the extent of this activity may differ depending on the malaria-causing agent, the bioavailability of R and Q post-digestion, and/or the pathways of transport for Q and R. Q is transported via the passive transcellular pathway, while R is transported using active carrier-mediated transport (Walgren et al., 1998). This may be due to the glycosidic nature of R (Hollman et al., 1999).

2.2.6 Prior Work

To quantify the AN and flavonoid content, after digestion but before adsorption into the bloodstream, a simulated digestion study was conducted using *A. annua* dried leaves (Weathers et al., 2014b). This study simulated the oral, gastric and intestinal phases of digestion. Table 2 shows how each phase of digestion was simulated.

Table 2: Methods used to simulate digestions of *A. annua* dried leaves

Digestion Phase	Method of Simulation
Oral	1. Vortex solution of 0.36 AN, 1.64 mL H_2O and □□amylase 2. Blanket solution with N_2 and cap 3. Place solution in 37° water bath for 10 minutes
Gastric	1. Place solution on ice 2. Add saline and adjust the pH to 4.0 with HCl 3. Blanket solution with N_2 and cap 4. Incubate for 60 min. at 90 opm
Intestinal	1. Place solution on ice 2. Adjust pH to 4.0 with $NaHCO_3$ 3. Add 0.5 mL $NaHCO_3$ and 0.75 mL bile extract 4. Adjust pH to 6.5, add saline and blanket with N_2 5. Place test tube in 37° water bath and incubate at 90 opm for 2 hours

The study examined how the leaves of *A. annua* digested with various food sources affected the bioavailability of AN and flavonoid content in the intestinal liquid. First the dried leaves were digested alone and AN and flavonoid levels were measured. Table 4 shows the results from this study. Undigested dried leaves contained approximately 7.6 mg/g DW of AN and about 2.9 mg/g DW of flavonoids. The AN and flavonoids recovered after each phase of digestion were less than the starting material. AN is assumed to be most bioavailable once it is released into the liquid of each digestion phase; only 22% of the starting AN was found in this phase (Weathers et al., 2014b; Table 3).

Table 3: Results from *A. annua* dried leaves digestion simulation (Weathers et al., 2014b)

Digested Leaves	Artemisinin Content (mg/g DW)		Flavonoids (mg/g DW)	
	Solid Phase	Liquid Phase	Solid Phase	Liquid Phase
Oral Phase	5.46	0.61	1.158	0.071
Gastric Phase	5.55	0.81	0.899	0.064
Intestinal Phase	2.24	1.72	0.983	0.087

Dietary components were then added to the dried leaves prior to digestion. The components tested and their relative impacts on AN and flavonoid level extracted from the intestinal phase of digestion are shown in Table 4. When dried leaves were combined with sucrose, canola oil, peanut oil or white rice the release of AN was not negatively affected. In addition, when dried leaves were combined with many of the dietary components the available flavonoid content in the intestinal liquid increased significantly. For sucrose and canola oil, the dried leaves contained 0.10 mg FLVs/g DW, whereas the sucrose and canola oil combined with

dried leaves contained <0.20 mg FLVs/g DW. Digestion in the presence of millet, cornmeal, however, reduced AN release into the liquid phase of the intestinal stage of digestion.

Table 4: Dietary components added to dried leaves and their effects on AN and flavonoid content

Dietary Component	Percent change from dried leaves digested alone	
	Artemisinin (%)	Flavonoids (%)
Sucrose	-8a	+105
Canola oil	-19a	+101
Red palm oil	-35a	+99
Sunflower oil	-41a	+132
Peanut oil	-6a	+59
White rice meal	-21a	+54
Corn meal	-58b	+103
Millet Meal	-42b	+15

Weathers et al. (2014b) further showed that, when digested, therapeutic compounds from dried leaves would likely be more bioavailable if administered as a tablet rather than in a capsule because both gelatin and cellulose capsules reduced AN availability. The next step in determining bioavailability of AN and flavonoids in *A. annua* is to determine the rate at which these compounds move across the intestinal epithelium. In studying the transport of these compounds *in vitro*, the Caco-2 cell line is often used.

2.3 Caco-2 Cells

The Caco-2 (ATCC® HTB37™) cell line is a line of human colorectal adenocarcinoma cells originally isolated from a Caucasian male, aged 72 years. Although there are many human colorectal adenocarcinoma cell lines, only two lines are closely related, in terms of structure and function, to the Caco-2 cell line. The HT-29 (ATCC® HTB-38™) line is a tumorigenic line derived from a Caucasian female aged 44 years, whereas the C2BBe1 [clone of Caco2] (ATCC® CRL2102™) cell line is a clonal line derived from Caco-2 cells. Though similar in function, neither HT-29 nor C2BBe1 express receptors and genes identical to Caco-2. These differences in protein expression cause physical differences, such as the multilayered monolayers that can be seen in HT-29 cultures (ATCC, 2012a; ATCC, 2012c). This makes HT-29 and CBBe1 unsuitable for use as a model system.

2.3.1 Characteristics and variability

The Caco-2 cell line (HTB-37) is characterized by epithelial-like morphology, with generally polygonal shape and adherent growth. (ATCC, 2012b, Figure 5). This adherent growth allows Caco-2 cells to form a confluent monolayer with tight intercellular junctions. Exponential

cell growth slows to a consistent, linear rate after approximately six days (Hidalgo et al., 1989). Upon reaching confluence, Caco-2 cells in culture differentiate into a monolayer that is polarized apically and basolaterally. These cells have a similar structure and function to that of enterocytes, which are the epithelial cells that line the intestines, making Caco-2 cells a good model for study of drug transport from the intestine into the blood stream.

Figure 5: Caco-2 cells in a confluent monolayer

Differentiated Caco-2 cells are characterized by the expression of heat stable enterotoxin, epidermal growth factor, and retinoic binding proteins I and II (Sun and Pang, 2008). Additionally, cell morphology is more similar to that of enterocytes, including the growth of microvilli (Hidalgo et al., 1989). To maintain a consistent expression of enterocytic structure and function, regular quality control must be conducted on the cultures (Hubatsch et al., 2007).

Without proper quality control, the Caco-2 cell line, with multiple passages may alter over time. Quality control is crucial to prevent the integrity of the cell monolayer from declining, which means that the cells would no longer form the tight intercellular junctions that make Caco-2 cells useful as a model system for the human intestine. After 70 passages, there is significant decline in membrane integrity (Briske-Anderson et al., 1996). For this reason, two primary quality control procedures exist to test the integrity of a Caco-2 monolayer: measurement of

trans-epithelial electrical resistance (TEER or TER), and diffusion of a known compound across the monolayer (Briske-Anderson et al., 1996).

TEER is a measurement of resistance of the cell monolayer to an electrical current. This is done using a TEER probe, which is attached to a voltmeter. To measure TEER, one probe is placed on the apical side of the monolayer, and a second probe is placed on the basolateral side of the monolayer. Using the reading on the voltmeter, the TEER can be calculated using the formula:

$$TEER\ value\ (ohm \cdot cm^2) = TEER\ measurement\ (ohms) * Area\ of\ membrane\ (cm^2)$$

If a TEER probe is not available, diffusion of a known compound across a Caco-2 monolayer can instead be used by tracking a radioactive compound, such as [^{14}C]mannitol, or a dye compound, such as Lucifer Yellow (Hubatsch et al., 2007; Himanshu, 2013). The integrity of the monolayer can be assessed by adding one of the above test compounds to the apical side of the monolayer and determining the permeability coefficient using the formula:

$$Permeability\ coefficient\ (^{cm}/_{s}) = \frac{\Delta Q}{\Delta t} * \frac{1}{A * C_0}$$

In this formula, $\frac{\Delta Q}{\Delta t}$ is the permeability rate, in µg/min, of a given compound, A is the surface area of the Caco-2 monolayer (cm^2), and C_0 is the initial concentration, in µg/mL, on the apical side of the monolayer (Augustijns et al., 1996). A permeability coefficient, P_{app}, of approximately 1.2 nm/s indicates a monolayer that is sufficiently confluent and is ready to be used in experiments (Hubatsch et al., 2007).

An alternative method for quality control using a dye compound is to measure the rejection, or lack of passage, of the compound through the Caco-2 monolayer. This is done by adding the fluorescent dye, Lucifer Yellow, on the apical side and measuring the relative fluorescence units (RFU) of the dye on the basolateral side. Percent rejection of Lucifer Yellow is assessed using the following formula:

$$\%\ Lucifer\ Yellow\ Rejection = 100 * \left(1 - \frac{RFU\ of\ Lucifer\ Yellow\ on\ basolateral\ side}{initial\ RFU\ of\ Lucifer\ Yellow\ added\ to\ apical\ side}\right)$$

The percent of Lucifer Yellow rejection should increase with culture time, as the Caco-2 monolayers become more confluent (Corning Life Sciences Incorporated, 2013; Himanshu, 2013).

Although it is useful to implement both TEER measurement and transport of a known compound as quality control methods, it is not necessary. It has been shown that increased TEER corresponds to increased Lucifer Yellow rejection, and vice versa (Hidalgo et al., 1989).

2.4 Drug Permeability and Transport Studies

The differentiation of Caco-2 cells into a functional enterocytic monolayer makes the Caco-2 cell line ideal for studies that require a model system that mimics the human intestinal epithelium. In particular, the Caco-2 monolayer can be used to study drug transport across the intestinal epithelium and thus predict drug absorption in humans (Artursson et al., 1996). The intestinal epithelium is the critical barrier to drug transport and absorption and, therefore, passage through the intestinal epithelium is the rate-limiting step in absorption of a drug (Hidalgo et al., 1989).

2.4.1 Drug Transport Pathways

There are four transport pathways across the intestinal epithelium: the passive transcellular pathway, the passive paracellular pathway, the active carrier-mediated transcellular pathway, and the transcytosis pathway (Artursson et al., 1996; Figure 6). In the passive transcellular pathway, indicated by arrow A in Figure 6, a given molecule passes through the semi-permeable membrane on the mucosal, or apical, side of a polarized enterocyte, passes through the cell, and passively diffuses across the cell membrane on the serosal, or basolateral side with no energy exerted by the cell. Similarly, in the passive paracellular pathway, B in Figure 6, a given molecule diffuses from mucosal to serosal side through the junction between two enterocytes. The third possible pathway, C in Figure 6, is the active, carrier-mediated pathway. Carrier-mediated transport involves a cellular carrier protein, a type of membrane transport protein, binding to the target molecule. The molecule-carrier complex then undergoes a

series of conformational changes in order to transfer the molecule across to the opposite membrane from which the molecule was accepted (Alberts et al., 2007, p. 653). The final pathway for transport across the intestinal epithelial membrane is the transcytosis pathway, D in Figure 6. In this pathway, specific molecules are recognized by receptors on the surface of the cell membrane, which then forms a vesicle around the molecule. This vesicle is then transported across the intracellular space until the vesicle fuses with the serosal-side membrane, releasing the molecule (Alberts et al., 2007, p. 797).

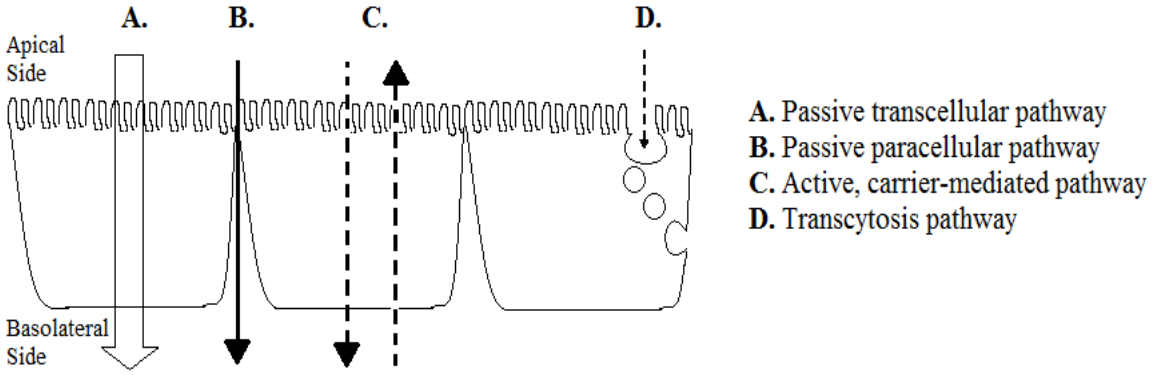

Figure 6: Drug transport pathways

Most drug compounds that are orally administered in humans are absorbed across the intestinal epithelium through the passive transcellular pathway (Fig. 6A; Artursson and Karlsson, 1991). Additionally, drug compounds that are hydrophilic or peptide-based are likely to pass through the passive paracellular pathway or the carrier-mediated pathway, (Fig. 6B and C, respectively) if their shape resembles that of cell nutrients. However, AN is neither peptidic nor hydrophilic, it is likely to cross the intestinal epithelium through the passive transcellular pathway. This assumption was supported by a study of AN transport through Caco-2 monolayers (Augustijns et al., 1996).

2.4.2 Transport of Artemisinin

To increase understanding of the oral absorption of AN and its more water-soluble analogue, sodium artesunate, a study of AN transport and absorption across Caco-2 monolaryers compared apical to basolateral (a → b) and basolateral to apical (b → a) transport of both compounds under different conditions (Augustijns et al., 1996). The permeability of AN was

significantly higher than sodium artesunate, with permeability coefficients (P_{app}) of 30.4 and 4.0 (x 10^{-6}) cm sec^{-1}, respectively (Table 5). Additionally, transport of AN across the Caco-2 monolayer did not significantly differ between a → b and b → a direction; P_{apps} were 30.4 and 30.9 (x 10^{-6}) cm sec^{-1}, respectively. Thus, AN must cross the monolayer through the passive transcellular pathway, rather than through active transport. This is further supported by little to no change in AN permeability when the temperature was decreased from 37 to 2°C, and also in the presence of sodium azide (Table 5). An active transport mechanism would be more temperature-dependent and subject to azide poisoning (Augustijns et al., 1996). From these data, it was concluded that although AN has low solubility in water, it readily crosses the intestinal epithelium through passive diffusion (Augustijns et al., 1996).

Table 5: Caco-2 permeability of AN under various conditions (Augustijns, 1996)

Conditions	T (°C)	P_{app} (x10^{-6}) (cm/s)	SD
Artemisinin (100 µM, 1 h)			
Apical to Basolateral Transport (a → b)	37	30.4	1.7
	20	22.5	0.5
	2	20.0	0.5
Basolateral to Apical Transport (b → a)	37	30.9	2.6
Sodium Azide (1 mM) (a → b)	37	30.8	1.9
Artesunate (10 mM, 1 h)			
pH 7.4 (a → b)	37	4.0	0.4

2.4.3 Ethanol in Drug Transport Studies

To effectively dissolve drug compounds for use in Caco-2 transport studies, the solubility of the drug compound must be evaluated. For compounds with low solubility in transport media, the use of organic solvents, such as ethanol, may be necessary. However, when using such solvents, it is important to note the potential for damage to the Caco-2 monolayers from extended exposure.

In human mast cells, which, like Caco-2 cells, occur in the gastrointestinal tract, exposure to 43 mM of ethanol for a period of four days reduced cell viability by approximately 40% (Nurmi et al., 2009). In addition to inducing apoptosis, exposure to ethanol can reduce the rate of proliferation of cells *in vitro*. A study in the human promyelocytic leukemia cell line, HL-60, showed that cells cultured with 0.5-4% ethanol in culture media, had a significantly lower proliferative rate after 24 hours of culture. However, after only 1 hour of culture, the different

ethanol concentrations did not have statistically different effects on cell proliferation (Mareková et al., 2000).

In studying drug transport across Caco-2 monolayers, an incubation of 1-2 hours is generally used (Hubatsch et al., 2007). Thus, the time in which the Caco-2 cells are exposed to a drug compound dissolved in ethanol is limited enough that massive apoptosis in the monolayer is unlikely. However, incubation with ethanol can cause morphological changes in the Caco-2 monolayers, namely the reduction of monolayer confluence (Moyes et al., 2010). A study by Moyes et al. (2010) on the effects of culture conditions on particle uptake by Caco-2 monolayers showed that a treatment of 10% ethanol in culture medium for 60 minutes reduced trans-epithelial resistance, a measure of monolayer confluence, by 23%.

It is clear that a 60 minute exposure of Caco-2 cells to 10% ethanol is damaging to the cell monolayer and will therefore affect the results of drug transport studies. For that reason, all concentrations of ethanol used to dissolve hydrophobic (low-solubility) drug compounds should be less than 10%. At any concentration used, there must be a control for ethanol exposure. For this, one or more transwells should be exposed for the entirety of the study to ethanol and transport medium, at the percentage of ethanol used for the actual transport experiment, after which the monolayer integrity should be evaluated. If needed, such a control could then be used to normalize the data collected from the drug transport studies to account for any drug transport that results from decreased monolayer integrity, rather than true transport across the Caco-2 monolayers.

3.0 Hypothesis

By using a Caco-2 monolayer to simulate drug transport across the intestinal epithelium, this study will establish the effect of Q and R on the transport of AN across the Caco-2 monolayer. If addition of either or both of compounds increase the P_{app} of AN, this would indicate that Q and/or R increase the bioavailability of AN on the serosal side of the monolayer.

Objectives:

1. Establish the model system for studying the transport of secondary plant metabolites across a Caco-2 monolayer.
2. Measure the transport of AN passage through a Caco-2 monolayer to replicate the study by Augustijns et al. (1996).
3. Measure the transport of AN + Q through a Caco-2 monolayer.
4. Measure the transport of AN + R through a Caco-2 monolayer.

4.0 Methodology

4.1 Cell Line & Maintenance

Human epithelial colorectal adenocarcinoma cell line, Caco-2 (HTB-37), was obtained from the American Type Culture Collection (ATCC). The culture conditions recommended by the ATCC were ambient air with 5% carbon dioxide at 37° C. The complete growth medium as recommended by the ATCC was Eagle's Minimum Essential Medium (EMEM) with 20% fetal bovine serum (FBS). Cells cultured in either 25 or 75 cm^2 T-flasks were maintained in EMEM with 20% FBS and 1% penicillin/streptomycin. Under these culture conditions, the population doubling time for Caco-2 cells is approximately 62 hours (American Type Culture Collection (ATCC), 2012b). Cells seeded onto transwell inserts were maintained in 10% FBS with 1% penicillin/streptomycin to promote differentiation. All cultures were fed and passaged as needed.

4.2 Creation of drug transport study model system using Caco-2 Monolayers

The permeability and absorption experimental setup of this study used the protocol described by Hubatsch et al. (2007). The Caco-2 cells were cultured on 12 mm semi-permeable polycarbonate transwell inserts that have a 0.4 µm pore size. Cells were seeded onto transwell inserts approximately three weeks before the experiment to allow the cells time to differentiate into confluent monolayers on the membrane.

For inoculation of transwells inserts, confluent Caco-2 cultures grown in 25 or 75 cm^2 T-flasks were first trypsinized. Cell culture medium was removed by aspiration. Cells were rinsed with Phosphate Buffered Saline (PBS). PBS was aspirated and a trypsin solution composed of 80% PBS, 10% edetic acid and 10% trypsin (10 x stock solution 2.5% (wt/vol)) was added. During trypsinization, cells were scraped off the culture surface with a cell scraper. The protease activity of trypsin, in combination with cell scraping, served to detach cells from the culture surface and one another. Once this is accomplished, the protease activity of trypsin was stopped by diluting the trypsin with culture medium (EMEM).

The cell suspension was then transferred to a 15 mL conical tube. The conical tube was centrifuged at 100 x g for three minutes, causing a pellet of cells to form at the bottom of the tube. After centrifugation, the supernatant in the tube was aspirated and the cell pellet resuspended in culture medium (EMEM). A 0.1 mL sample of the cell suspension was taken to count viable cells. An aliquot of 0.1 mL of 4% solution of trypan blue was added to the sample, which was then pipetted into a hemocytometer. When viewed under a microscope, cells that have

turned blue were not considered viable. To continue with the experiment, at least 95% of the cells must be viable (Strober, 2001).

At this point, a hanging transwell insert of 1.92 cm^2 area (Corning Inc., Product #3401) was placed in each well of a 12-well, culture plate (Corning Inc., Product #3513), wetted with 0.1 mL of EMEM and left for two minutes. The cells were then seeded by pipetting the necessary volume of cell suspension to achieve 300,000 live cells onto each transwell insert. Culture medium was added to bring the volume to 0.5 mL. Immediately afterwards, the basolateral chamber was filled with 1.5 mL of culture medium and the well plates were incubated at 37°C for three weeks. Every third day during this period, the medium from both the basolateral and apical sides was aspirated and replaced with 0.5 mL and 1.5 mL of EMEM, respectively.

Before drug transport studies were performed, a confluence check was completed using the standard operating procedure for Lucifer Yellow assays as detailed in Appendix B. If the Lucifer Yellow assay resulted in a Lucifer Yellow rejection of approximately 80% or greater, the Caco-2 monolayers were considered sufficiently confluent for use in drug transport studies. For drug transport studies, the solution to be placed on the apical side was warmed to 37°C. This solution was composed of phosphate buffered saline (PBS) and certain dissolved compounds, depending on the particular experiment. The compounds may be AN, FLVs, or a combination of these. When the solutions were prepared, the transwell inserts were transferred to new 12-well plates containing PBS on the basolateral side and 0.5 mL of PBS + compound solution added to the apical side of the monolayer. A zero time sample was taken from the solution on the apical side. The well plates were then incubated at 37°C for 60 minutes. At 15 minute intervals, the transwell inserts were transferred to new well plates containing 1.5 mL fresh PBS on the basolateral side. The media remaining in each well plate was extracted. A final sample was also taken from the apical chamber at 60 minutes.

4.3 Transport of test compounds across a Caco-2 monolayer

To measure the amount of AN that passes through a Caco-2 monolayer, apical to basolateral transport experiments were performed as described by Hubatsch, et al. (2007) and modified to suit the transport of AN. To maintain sink conditions, meaning that concentration of compound on the basolateral side does not exceed 10% of that of the apical side, during the transport experiment, the transwell inserts were transferred to fresh 12-well plates containing

PBS every fifteen minutes for one hour, as suggested by Augustijns, et al. (1996) and Hubatsch et al. (2007). Because the transwell inserts were transferred to new well plates every fifteen minutes for one hour, the basolateral medium in the used well plates was extracted for quantification of AN by Gas Chromatography – Mass Spectrometry (GC/MS).

Table 6 describes the experimental set-up for transport of AN ± Q or R. All stock solutions of AN, Q and R were made in 70% ethanol. For the AN studies, a small aliquot of 70% ethanol was added to maintain a constant volume of ethanol throughout all studies. The AN stock solution was 7.08 mM to yield 177.09 µM of AN in each transwell, as described in Table 6.

Table 6: Experimental design for apical transport media

Experimental Treatment	Volumes for Transport Medium (µL)			Amount of Compound per Transwell (µg)	Concentration of Compound per Transwell (µM)
	Stock Solution	70% Ethanol	PBS		
AN	12.5 AN	12.5	475	25 AN	177.09 AN
AN + Q	12.5 AN	0	475	25 AN	177.09 AN
	12.5 Q			15 Q	99.26 Q
AN + R	12.5 AN	0	475	25 AN	177.09 AN
	12.5 R			30 R	98.28 R

To measure the amount of AN that passed through a Caco-2 monolayer in conjunction with Q, a similar method was used to that described for the transport of pure AN, modified to include Q in the transport experiment. Table 6 describes the experimental set-up for AN + Q studies. As with transport of AN alone, 12.5 µL of a 7.08 mM AN stock solution was used in transport medium. Additionally, 12.5 µL of a 3.97 mM Q stock solution made in 70% ethanol was added, yielding a concentration of 99.26 µM Q in each transwell insert.

For AN + R studies, we followed the method as described for the transport of pure AN, but modified to also include R in the transport medium. Similar to the AN + Q studies, 12.5 µL of R stock solution were added to the transport media. To maintain equal molarity of both Q and R, the stock solution of R was 3.93 mM, yielding a concentration of 98.28 µM R per transwell insert, as shown in Table 6. The distribution of experimental treatments in a 12 well plate is shown in Figure 7.

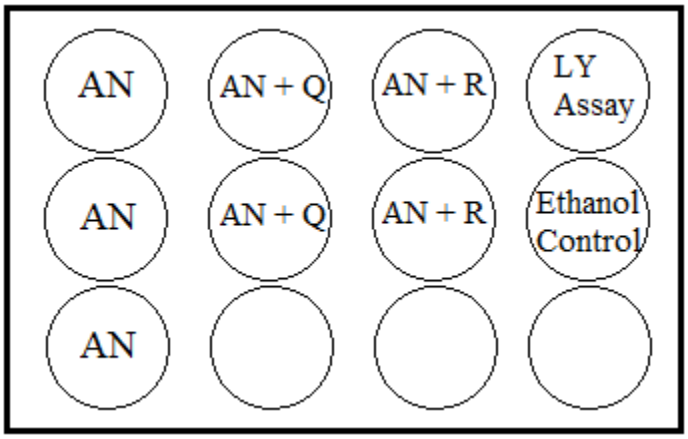

Figure 7: 12-Well plate experimental set-up diagram

4.4 Quantification of artemisinin and flavonoid passage through the Caco-2 monolayer

Upon completion of each transport experiment, the medium from each well in every used well plate was immediately extracted with an equal volume of methylene chloride. The extracted samples were dried under N_2 gas, resuspended in a known volume of methylene chloride, and a known aliquot was transferred to GC/MS vials. The amount of AN in each sample was quantified using the method of Weathers and Towler (2012).

4.5 Statistical Analysis

There were three replicates of the AN studies, and two replicates each of the AN + Q and AN + R studies (Figure 7). To determine statistical significance of data between AN and AN + either Q or R, a Student's T-Test was performed.

5.0 Results

5.1 Lucifer Yellow Validation of Caco-2 Monolayers

To test the integrity of the Caco-2 monolayers, a single transwell insert was used in a representative Lucifer Yellow (LY) assay. The LY assay resulted in a percent LY rejection of 75.52%. Although <80% this percentage was deemed sufficiently confluent to proceed with this preliminary transport study. Another transwell insert was used to control for any damage caused by exposure of the Caco-2 monolayers to 5% ethanol present in all studies. This LY assay resulted in an LY rejection of 83.60%, indicating no significant damage from exposure to 5% ethanol for 60 minutes and was consistent with the LY assay of the well lacking ethanol. The raw data for these LY assays are shown in Appendix F.

5.2 Apical to Basolateral AN Transport

First, AN a→b transport was measured. The average concentration of AN on the basolateral side of transwell inserts for AN transport every fifteen minutes was not statistically different and ranged from an average of 0.4 µg/mL to 0.18 µg/mL at 60 minutes (Figure 8A). When Q was added with AN, there was not statistical difference from AN alone at each sampling time and the AN concentration at each time point ranged from 0.4 µg/mL to 0.3 µg/mL (Figure 8B). Similarly, there was no statistical difference between AN alone and AN + R, in which the AN concentration at each sampling time ranged from 0.5 µg/mL to 0.6 µg/mL (Figure 8C).

When Q was added to AN, its presence appeared to not only increase overall average AN concentration after 30 minutes, but seemed to result in more consistent AN passage across all time points (Figure 8B). Similarly, the presence of R also appeared to increase AN transport (Figure 8C). When the cumulative basolateral concentration of AN was measured, the rate of AN transport for the AN, AN + Q, and AN + R studies is shown in Figure 9. The orange and grey lines representing AN + Q and AN + R transport, respectively, indicate greater AN transport after 45 and 60 minutes than was seen in the blue line, which represented AN transport alone (Figure 9). However, only AN + R was significantly greater at 60 minutes. Indeed, the rate of AN transport ± Q or R was the same between 0 and 15 minutes (Figure 9). The transport of AN alone appeared to be bimodal; between 0 and 15 minutes the rate of change in AN concentration was 0.0203 µg mL^{-1} min^{-1}, about four times faster than the rate of change, 0.0055 µg mL^{-1} min^{-1}, between 15 and 60 minutes (Figure 10A).

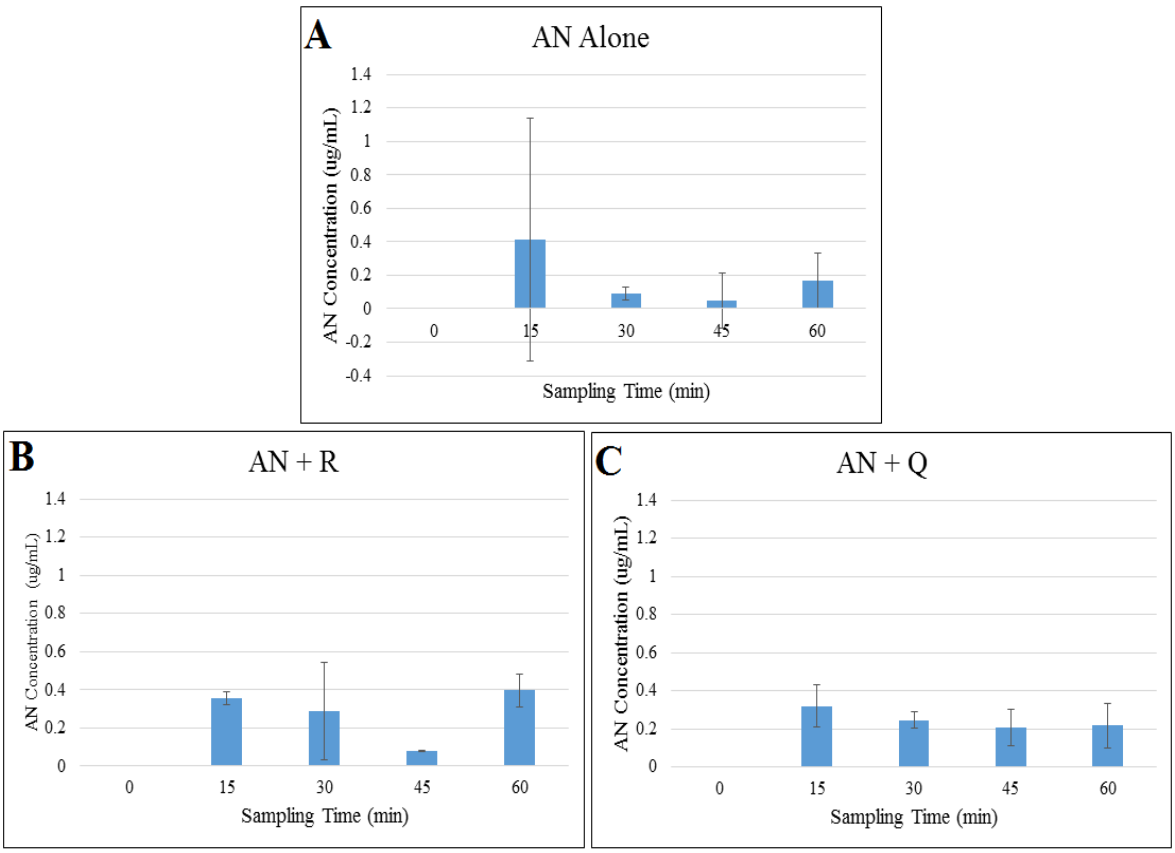

Figure 8: Average Basolateral Concentration of AN ± Q or R over 60 minutes. A, AN alone; B, AN + Q; C, AN + R.

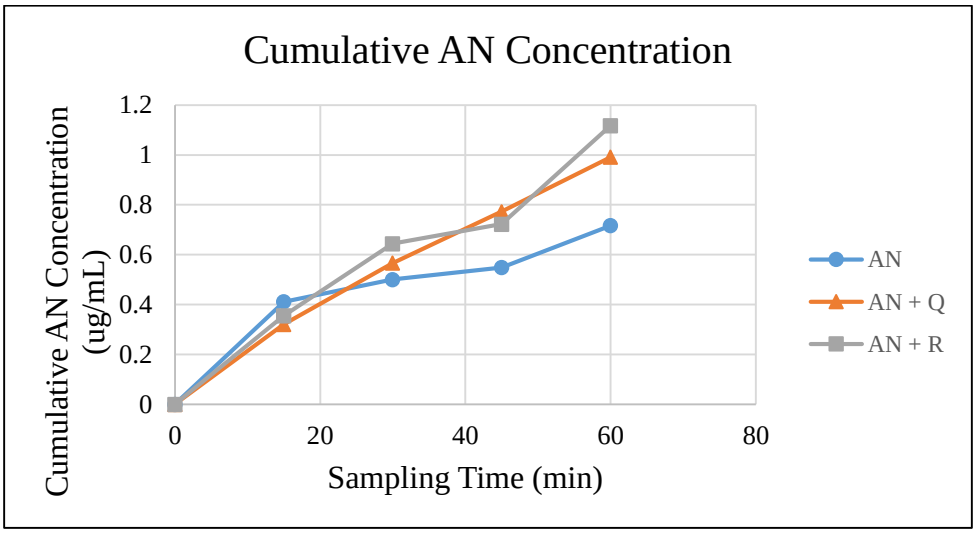

Figure 9: Cumulative AN concentration at 15-minute time points in all transport studies

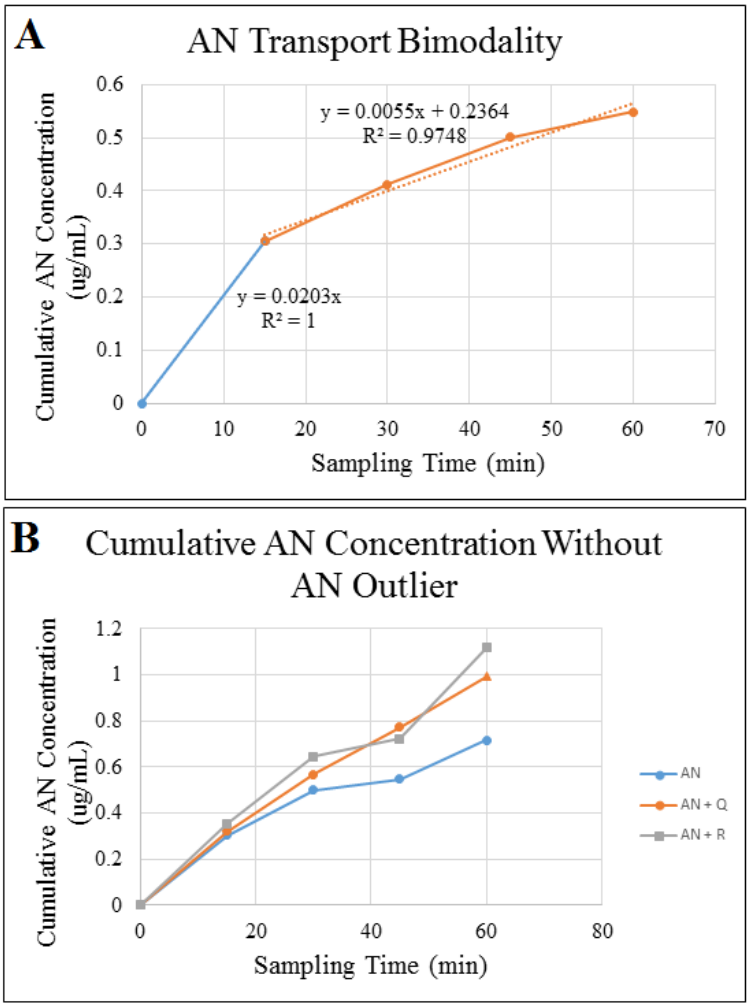

Figure 10: Change in permeability rate of AN transport

The appearance of bimodality may be influenced by the presence of an outlier at 15 minutes. Although when the outlying value was removed, bimodal AN transport was not as apparent, there was still a decline in the rate of change in AN concentration from 0.016 µg mL^{-1} min^{-1} between 0 and 30 minutes to 0.0073 µg mL^{-1} min^{-1} from 30 to 60 minutes. (Figure 10B).

5.2.1 Permeability Coefficient

Using the average total amount of AN transported across the Caco-2 monolayers over 60 minutes, the permeability coefficient (P_{app}) for AN was calculated for AN, AN + Q, and AN + R studies using the equation shown in the methods. The permeability coefficient for AN alone was 7.06 x 10^{-6} cm/s, which was not statistically different from that of AN + Q, which was 11.75 x 10^{-6} cm/s. However, the permeability coefficient for AN + R, 12.65 x 10^{-6} cm/s, was statistically different from AN alone (Table 7).

Table 7: Permeability coefficient of AN for all studies

Experimental Treatment	P_{app} (cm/s) ($x10^{-6}$)
AN	7.06a
AN + Q	11.75a
AN + R	12.65b

Both AN + Q and AN + R yielded greater P_{app} values than AN alone, with a percent change between AN and AN + Q of 66.43%, while the percent change between AN and AN + R was 79.18%.

6.0 Discussion

In studying the transport across Caco-2 monolayers of AN alone, it was expected that a permeability coefficient P_{app} of approximately 30.4 x 10^{-6} cm s^{-1} would result from a 60 minute transport study at 37º C, as reported by Augustijns et al. (1996). Such a result would indicate that AN was, as previously shown, successfully transported across Caco-2 monolayers through the passive transcellular pathway (Augustijns et al., 1996). Rather than using 24 mm transwell inserts used by Augustijns et al. (1996), this study used 12 mm inserts for culturing Caco-2 monolayers, so there was a cross-sectional area of 1.22 cm^2. However, because the permeability coefficient (P_{app}) was normalized to the growth surface area of the transwell, it was possible to compare the two results. Augustijns et al. (1996) reported that the P_{app} of AN was 30 cm/s (x 10^{-6}). The P_{app} for AN in this study was 7.06 cm/s (x 10^{-6}), about 24% of the earlier study.

Similar to AN, Q is also transported across Caco-2 monolayers using the passive transcellular pathway (Walgren et al., 1998). Q also was shown to act synergistically with AN, so it was expected that AN transport across Caco-2 monolayers would be enhanced by the presence of Q (Hollman et al., 1996). As expected, when AN + Q was used in apical to basolateral transport studies, not only the rate, in terms of P_{app}, but the total amount of AN that crossed the Caco-2 monolayers increased, but neither value was statistically different from that of AN alone.

In contrast to the passive transport of AN and Q, R was shown to be successfully transported across Caco-2 monolayers in a time- and dose-dependent manner using the active carrier-mediated transport (Zhang et al., 2013). *In vitro* experiments also showed that R was less bioavailable than Q after oral administration (Erlund et al., 2000). Rather, serosal levels of Q were shown to increase after ingestion of R, indicating that R, rather than being actively transported as was shown *in vitro*, is hydrolyzed into Q to facilitate transport through the intestinal lumen (Erlund et al., 2000). To our knowledge, R has not been specifically shown to act synergistically with AN. However, because it does travel across a Caco-2 monolayer and may be cleaved into Q to facilitate transport, R was also hypothesized to increase transport of AN across Caco-2 monolayers, with an increase in apical to basolateral P_{app} for AN. Though because R is less bioavailable any increase was anticipated to be less than that for AN + Q. However, the increase in P_{app} seen when R was added with AN was statistically different from that of AN alone, although the total amount of AN transported was not. This difference in rate of AN

transport was most evident between 45 and 60 minutes. Based on the observed permeability coefficients for AN + Q and AN + R, the results suggest that R may enhance AN transport.

Q and R are related compounds, in that Q is the aglycone of R, yet only R significantly increased the rate AN transport. This suggested that the rutinose sugars in R may facilitate active transcellular transport of AN (Hollman et al., 1999). The apparent increase in P_{app} for AN may also be due to the transport of R through the active carrier-mediated pathway (Erlund et al., 2000). It is unknown whether R was hydrolyzed to Q during incubation, as although samples were analyzed for R and Q, the two compounds are difficult to differentiate using GC/MS, as they have the same elution time and the same ion signature.

The P_{app} for AN alone could also be affected by the observed bimodality in AN transport. The permeability rate for AN alone between 0 and 15 minutes was 0.014 µg/mL greater than the rate between 15 and 60 minutes, a 25% increase compared to the later stage of the transport study.

7.0 Conclusions and Future Studies

In this study, flavonoids Q and R increased the rate of AN transport. Although from these data only AN + R was significantly different from AN transport alone, sample size was two, so it is possible that with a larger sample size, the AN + Q results could also be significant. Therefore, it is recommended that the studies of AN in combination with Q and R be further replicated to increase the overall sample size for statistical analysis.

This *in vitro* study of AN transport suggested that flavonoids may affect pACT function by improving AN bioavailability. However, compounds such as other flavonoids, monoterpenes, and coumarins found in *A. annua* may also increase AN transport and should also be studied using apical to basolateral transport across Caco-2 monolayers. Additionally, b→a studies with AN could provide insight into the mechanism of AN transport. In an *ex vivo* study by Weathers et al. (2014b), sucrose was found to have no effect on AN in the intestinal liquid fraction. However, sugars may affect AN transport *in vitro*, as seen in the rutionse sugars of R. Therefore, it is recommended that AN transport in the presence of sugars be studied using Caco-2 monolayers. Specifically addition of either rhamnose or glucose or both should be included to determine their affect on AN + Q transport.

Another variable that should be examined is that of concentration. In contrast to the passive transport of AN and Q, R was shown to be successfully transported across Caco-2 monolayers in a time- and dose-dependent manner through active carrier-mediated transport (Zhang et al., 2013). Because R significantly increased AN transport at 98.28 µM, it is recommended that different concentrations of R be studied to determine whether higher or lower concentrations alter the assistance of AN transport across Caco-2 monolayers. Additionally, a longer period of study for transport experiments and/or increased sampling of the basolateral media is recommended to determine the effect of time in Q and R assistance of AN transport.

For the purposes of examining the effects of flavonoids on the bioavailability of AN, a model system was created with Caco-2 cells, which mimicked the human intestinal epithelium, a critical component in this and future transport studies. In doing this, pertinent standard operating procedures (SOP) were developed (Appendix A-G). These SOPs were specific to transport studies using Caco-2 cells on 12 mm transwell inserts and were developed through both research and experimental trials. Additionally, several protocols are recommended for future work with this model system. When culturing cells prior to transwell seeding, EMEM media with 20% FBS

is recommended to accelerate cell proliferation. In contrast, when seeding and incubating Caco-2 monolayers on transwell inserts, EMEM media with 10% FBS is recommended to promote cell differentiation. Once seeded onto transwell inserts, Caco-2 monolayers should be incubated for a minimum of three weeks before transport studies are performed. This allows monolayers to become fully confluent, as a three-week incubation yields an average percent LY rejection of 80%. During this incubation period, minimal transport of the cultures is recommended to reduce the risk of contamination. With these recommendations, a successful model system for AN transport studies can be created.

References

ATCC (American Type Cultural Collection). (2012a). ATCC product sheet C2BBe1 [clone of Caco2] (ATCC® CRL2102 ™) [Internet]. American Type Cultural Collection. Available from: http://www.atcc.org/~/ps/CRL-2102.ashx. Web. Accessed: 3 September 2013.

ATCC (American Type Cultural Collection). (2012b). ATCC product sheet Caco-2 (ATCC® HTB37 ™) [Internet]. American Type Culture Collection. Available from: http://www.atcc.org/~/ps/HTB-37.ashx. Web. Accessed: 3 September 2013.

ATCC (American Type Cultural Collection). (2012c). ATCC product sheet HT29 (ATCC® HTB38 ™) [Internet]. American Type Culture Collection. Available from: http://www.atcc.org/~/ps/HTB-38.ashx. Web. Accessed: 3 September 2013.

Alberts B, Johnson A, Lewis J, Raff M, Roberts K, Walter P. (2007). Molecular Biology of the Cell. New York, NY: Garland Science, Taylor & Francis Group, LLC. p. 653-797.

Artursson P, Karlsson J. (1991). Correlation between oral drug absorption in humans and apparent drug permeability coefficients in human intestinal epithelial (Caco-2) cells. Biochemical and Biophysical Research Communications 175(3):880-885.

Artursson P, Palm K, Luthman K. (1996). Caco-2 monolayers in experimental and theoretical predictions of drug transport. Advanced Drug Delivery Reviews 22(1-2):67-84.

Augustijns P, D'Hulst A, Van Daele J, Kinget R. (1996). Transport of artemisinin and sodium artesunate in Caco-2 intestinal epithelial cells. Journal of Pharmaceutical Sciences 85(6):577-579.

Azevedo M, Pereira A, Nogueria R, Rolim F, Brito G, Wong D, Lima-Junior R. (2013, October 23). The antioxidant effects of the flavonoids rutin and quercetin inhibit oxaliplatin-induced chronic painful peripheral neuropathy. Molecular Pain, 9(53).

Barry, D. (2010). Life Cycle of the Malaria Parasite in Human. [Internet]. Howard Hughes Medical Institute. Available from: http://www.hhmi.org/biointeractive/malaria-human-host. Web. Accessed: 4 September 2013.

Bhakuni RS, Jain DC, Sharma RP, Kumar S. (2001). Secondary metabolites of *Artemisia annua* and their biological activity. Current Science 80(1):35-48.

Bloland, PB. (2001). Drug resistance in malaria [Internet]. World Health Organization. Available from: http://www.google.com/url?sa=t&rct=j&q=&esrc=s&source=web&cd=2&cad=rja&uact=8&ved=0CDQQFjAB&url=http%3A%2F%2Fwww.who.int%2Fcsr%2Fresources%2Fpublications%2Fdrugresist%2Fmalaria.pdf&ei=3d9fU-WZMbbMsQSMiIDoDQ&usg=AFQjCNFlhz8wNrs63Sw_bsQwuSFVlpTtfg&bvm=bv.65397613,d.cWc. Web. Accessed 6 September 2013.

Bourgard F, Gravot A, Milesi S, Gontier E. (2001). Production of plant secondary metabolites: a historical perspective. Plant Science 161(5):839-851.

Brisibe E, Brisibe F, Ferreira JF, Magalhaes PM, Uyoh EA. (2008). Building a golden triangle for the production and use of artemisinin derivatives against falciparum malaria in Africa. African Journal of Biotechnology 7(25):4884-4896.

Briske-Anderson MJ, Finley JW, Newman SM. (1996). The influence of culture time and passage number on the morphological and physiological development of Caco-2 cells. Proceedings of the Society for Experimental Biology and Medicine 214:248-257.

CDC (Centers for Disease Control). (2012). Malaria [Internet]. Centers for Disease Control and Prevention. Available from: http://www.cdc.gov/malaria/index.html. Web. Accessed:7 September 2013.

Corning Incorporated. (2007). Corning HTS Transwell-96 Permeable Support Protocols for Drug Transport. Lowell, MA.

Elfawal MA, Towler MJ, Reich NG, Golenbock D, Weathers PJ. (2012). Dried whole plant *Artemisia annua* as an antimalarial therapy. PLoS ONE 7(12) e52746.

Elford BC, Roberts MF, Phillipson JD, Wilson RJ. (1987). Potentiation of the antimalarial activity of qinghaosu by methoxylated flavones. Transactions of the Royal Society of Tropical Medicine and Hygiene 81:434-436.

Erlund, I, Kosonen T, Alfthan G, Mäenpää J, Perttunen K. (2000). Pharmacokinetics of quercetin from quercetin aglycone and rutin in healthy volunteers. European Journal of Clinical Pharmacology 56: 545-53.

Ferreira JFS, Luthria DL, Sasaki T, Heyerick A. (2010). Flavonoids from *Artemisia annua* L. as antioxidants and their potential synergism with artemisinin against malaria and cancer. Molecules 15: 3135-70.

Freshney, RI (1994). Culture of Animal Cells: A Manual of Basic Techniques, 3rd edition. New York, NY: Alan R. Liss, Inc.

Ganesh D, Fuehrer H, Starzengruber P, Swoboda P, Khan W, Reismann J, Mueller M. (2012). Antiplasmodial activity of flavonol quercetin and its anologues in *Plasmodium falciparum*: evidence from clinical isolates in Bangladesh and standardized parasite clones. Parisitology Research 110(6): 2289-2295.

Guerra CA, Snow RW, Hay SI. (2006). Mapping the global extent of malaria in 2005. TRENDS in Parasitology 22(8):353-358.

Guo D, Wang Y, Wu T. (2012). Investigation of glandular trichome proteins in *Artemisia annua* L. using comparative proteomics. Public Library of Science 7(8):1-10

Harrison G. (1978). Mosquitoes, malaria, and man: A history of the hostilities since 1880. New York: Dutton.

Hay SI, Guerra CA, Tatem AJ, Noor AM, Snow RW. (2004). The global distribution and population at risk of malaria: past, present, and future. The Lancet: Infectious Diseases 4:327-336.

Hidalgo IJ, Raub TJ, Borchardt RT. (1989). Characterization of the human colon carcinoma cell line (Caco-2) as a model system for intestinal epithelial permeability. Gastroenterology 96(3):736-749.

Himanshu R, Jakir P, Pradnya H, Suneel P, Rahul S. (2013). The impact of permeability enhancers on assessment for monolayer of colon adenocarcinoma cell line (Caco-2) used in *in vitro* permeability assay. Journal of Drug Delivery & Therapeutics 3(3):20-29.

Hollman, P.C.H.; Gaag, M.V.D.; Mengelers, M.J.B.; Van Trijp, J.M.P.; De Vries, J.H.M.; Katan, M.B (1996). Absorption and disposition kinetics of the dietary antioxidant quercetin in man. Free Rad. Biol. Med. 21:703-707.

Hubatsch I, Ragnarsson EG, Artursson P. (2007). Determination of drug permeability and prediction of drug absorption in Caco-2 monolayers. Nature Protocols 2(9):2111-2119.

Kew Royal Botanical Gardens. *Artemisia annua* (sweet wormwood) [Internet]. Kew Royal Botanical Gardens. Available from: http://www.kew.org/plants-fungi/Artemisia-annua.htm. Web. Accessed: 1 October 2013.

Kim H, Lee D, Lim S. (2007). In vitro antimalarial activity of flavonoids and chalcones. Bulletin of the Korean Chemical Society. 28(12):2495.

Lawrence Berkeley National Laboratory. Malaria: What is it? [Internet]. Available from: http://www.lbl.gov/MicroWorlds/xfiles/malariawhatis.html. Web. Accessed: 25 March 2014.

Lehane AM, Saliba K, J. (2008). Common dietary flavonoids inhibit the growth of the intraerythrocyic malaria parasite BMC Research Notes 1(26):1-5.

Life Technologies. Trypan Blue Exclusion [Internet]. Life Technologies. Available from: http://www.lifetechnologies.com/us/en/home/references/gibco-cell-culture-basics/cell-culture-protocols/trypan-blue-exclusion.html. Web. Accessed: 2 October 2013.

Liu C-C, Yang S-L, Roberts MF, Elford BC, Phillipson JD. (1992). Antimalarial activity of *Artemisia annua* flavonoids from whole plants and cell cultures. Plant Cell Reports 11:637-640.

Mareková, M, Vávrová J, Vokurková D. (2000). Ethanol induced apoptosis in human HL-60 cells. General Physiology and Biophysics 19:181-94.

Meshnick SR. (2002). Artemisinin: mechanisms of action, resistance, and toxicity. International Journal of Parasitology 32:1655-1660.

Moyes, SM, Morris JF, Carr, KE. (2010). Culture conditions and treatments affect Caco-2 characteristics and particle uptake. International Journal of Pharmaceutics 387:7-18.

Mueller MS, Karhagomba IB, Hirt HM, Wemakor E (2000). The potential of *Artemisia annua* L. as a locally produced remedy for malaria in the tropics: agricultural, chemical and clinical aspects. J Ethnopharmacol 73:487-493

Mueller MS, Runyambo N, Wagner I, Borrmann S, Dietz K, Heide L (2004) Randomized controlled trial of a traditional preparation of *Artemisia annua* L. (Annual Wormwood) in the treatment of malaria. Trans R Soc Trop Med Hyg 98:318-321

Mutabingwa TK. (2005). Artemisinin-based combination therapies (ACTs): best hope for malaria treatment but inaccessible to the needy! Acta Tropica 95(3):305-315.

Nurmi, K, Methuen T, Mäki T, Lindstedt KA, Kovanen PT. (2009). Ethanol induces apoptosis in human mast cells. Life Sciences 85:678-684.

Pietta P. (2000). Flavonoids as antioxidants. Journal of Natural Products 63(7):1035-1042.

Rosenthal PJ. (2008). Artesunate for the Treatment of Severe Falciparum Malaria. The New England Journal of Medicine 358(17):1829.

Sachs J, Malaney P. (2002). The economic and social burden of malaria. Nature 415:680-685.

Sigma-Aldrich. (2013a). Artemisinin [Internet]. Sigma-Aldrich. Available from: http://www.sigmaaldrich.com/catalog/product/sigma/361593?lang=en®ion=US. Web. Accessed: 29 September 2013.

Sigma-Aldrich. (2013b). Quercetin [Internet]. Sigma-Aldrich. Available from: http://www.sigmaaldrich.com/catalog/product/sigma/q4951?lang=en®ion=US. Web. Accessed: 29 September 2013.

Stratton L, O'Neil MS, Kruk ME, Bell ML. (2008). The persistent problem of malaria: Addressing the fundamental causes of a global killer. Social Science & Medicine 67(5):854-862.

Strober W. (2001). Trypan blue exclusion test of cell viability. Current Protocols in Immunology 21:A.3B.1-A.3B.2.

Sun H, Pang K. (2008). Permeability, transport, and metabolism of solutes in Caco-2 cell monolayers: A theoretical study. Drug Metabolism and Disposition 36(1):102-123.

Taiz L, Zeiger E. (2006). Plant Physiology. Sunderland, MA: Sinauer Associates, Inc.

Tu Y. (2011). The discovery of artemisinin (quighaosu) and gifts from Chinese medicine. Nature Medicine 17(10):1217-1220.

van Zyl RL, Seatlholo ST, van Vurren SF. (2006). The biological activities of 20 nature identical essential oil constituents. Journal of Essential Oil Research 18:129-133.

Wade, L. G. (2010). Organic Chemistry (7th ed.). Upper Saddle River, NJ: Prentice Hall.

Walgren RA, Walle UK, Walle T. (1998). Transport of quercetin and its glucosides across human intestinal epithelial Caco-2 cells. Biochemical Pharmacology 55: 1721-27.

Weathers PJ, Arsenault PR, Covello PS, McMickle A, Teoh KH, Reed DW. (2010). Artemisinin production in *Artemisia annua*: Studies *in planta* and results of a novel delivery method for treating malaria and other neglected diseases. Phytochemistry Reviews 10:173-183.

Weathers PJ, Towler MJ. (2012). The flavonoids casticin and artemetin are poorly extracted and are unstable in an *Artemisia annua* tea infusion. Planta Medica 78:1024-1026.

Weathers PJ, Elfawal MA, Towler MJ, Acquaah-Mensah, GK, Rich SM. (2014a). Pharmacokinetics of artemisinin delivered by oral consumption of *Artemisia annua* dried leaves in healthy vs. *Plasmodium chabaudi*-infected mice. Journal of Ethnopharmacology pp 1-5.

Weathers PJ, Jordan NJ, Lasin P, Towler MJ. (2014b). Simulated digestion of dried leaves of *Artemisia annua* consumed as a treatment (pACT) for malaria. Journal of Ethnopharmacology 15(2014):858-863.

Weathers PJ, Reed K, Hassanali A, Lutgen P, Engeu PO (2014c) Chapter 4: Whole plant approaches to therapeutic use of Artemisia annua L. (Asteraceae). IN: *Artemisia annua*. - Pharmacology and Biotechnology. Eds., T Aftab, JFS Ferreira, MMA Khan, M Naeem Springer, Heidelberg, GDR pp. 51-74

WHO (World Health Organization). (2012). Guidelines for the treatment of malaria [Internet]. World Health Organization. Web. Accessed: 15 September 2013.

WHO (World Health Organization). (2013). Withdrawal of oral artemisinin-based monotherapies [Internet]. World Health Organization. Available from: http://www.who.int/malaria/areas/treatment/withdrawal_of_oral_artemisinin_based_monotherapies/en/index.html. Web. Accessed: 15 September 2013.

Wikimedia. (2011a). Artemisinin skeletal [Internet]. Wikimedia Commons. Available from: http://commons.wikimedia.org/wiki/File:Artemisinin_skeletal.svg. Web. Accessed: 29 September 2013.

Wikimedia. (2007a). Artemether [Internet]. Wikimedia Commons. Available from: http://commons.wikimedia.org/wiki/File:Artemether.svg. Web. Accessed: 29 September 2013.

Wikimedia. (2007b). Artesunate [Internet]. Wikimedia Commons. Available from: http://commons.wikimedia.org/wiki/File:Artesunate.svg. Web. Accessed: 29 September 2013.

Wikimedia. (2007c). Artemotil [Internet]. Wikimedia Commons. Available from: http://commons.wikimedia.org/wiki/File:Artemotil.svg. Web. Accessed: 29 September 2013.

Wikimedia (2009). Rutin structure [Internet]. Wikimedia Commons. Available from: http://commons.wikimedia.org/wiki/File:Rutin_structure.svg. Web. Accessed: 17 February 2014.

Wu T, Wang Y, Guo D. (2012). Investigation of glandular trichome proteins in *Artemisia annua* L. using comparative proteomics. PLoS ONE 7(8).

Zhang, X, Song J, Shi X, Miao S, Li Y. (2013). Absorption and metabolism characteristics of rutin in Caco-2 cells. The Scientific World Journal (2013):1-8.

Appendices

Appendix A: Treatment algorithm for malaria (CDC, 2012).

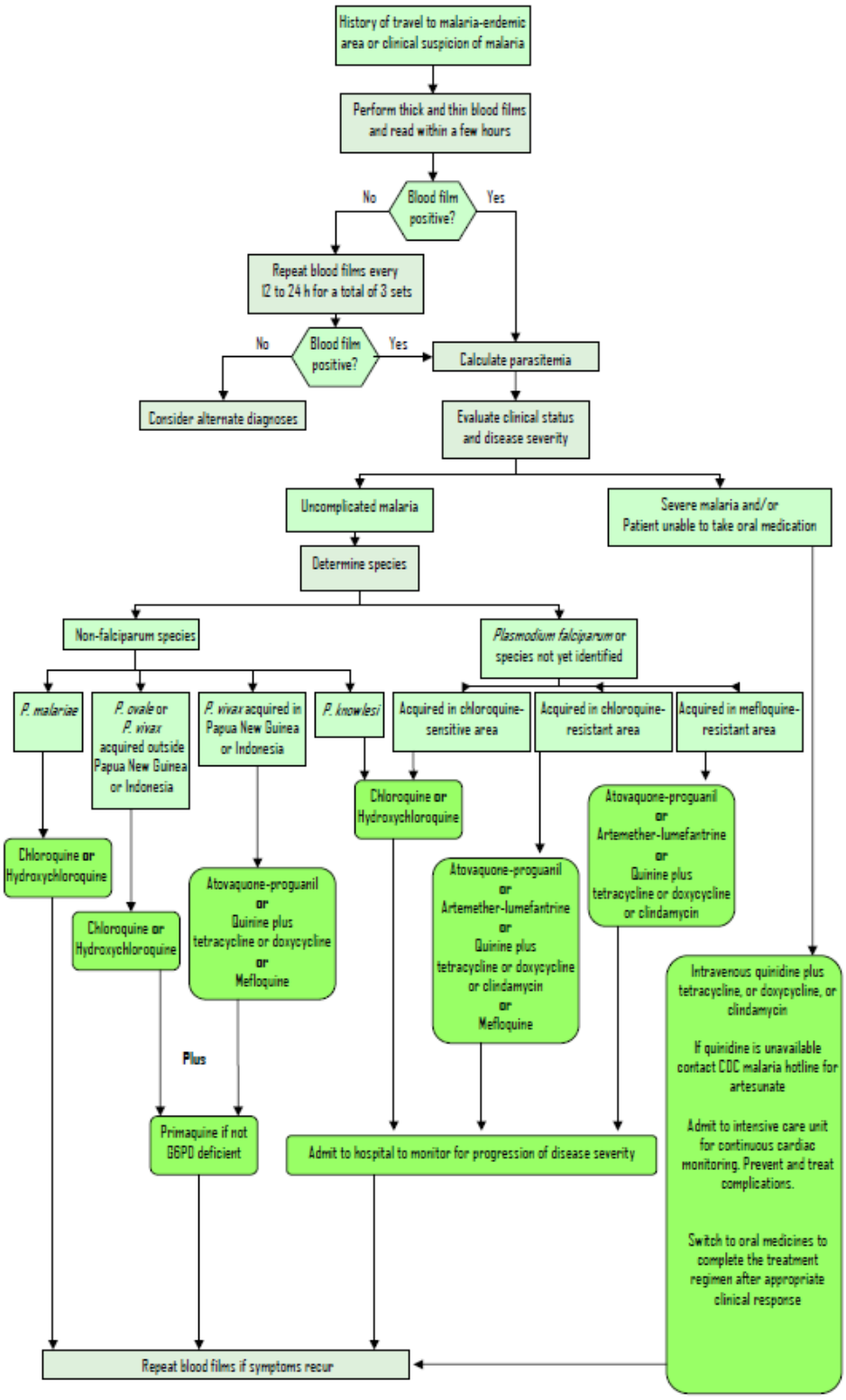

Appendix B: Standard Operating Procedure for Lucifer Yellow Assay

This SOP was modified from the Corning HTS Transwell-96 Permeable Support Protocols for Drug Transport, available from Corning, Inc. Lucifer Yellow (LY) is a fluorescent dye with low permeability that can travel across a cell monolayer only via paracellular diffusion, meaning diffusion through the gaps between cells. Thus, LY is not able to pass through when the cells have tight junctions, i.e., when the monolayer is fully confluent. A Papp between 5 and 12 nm/s or a 90% LY rejection is indicative of well-established monolayers. The following steps are used to prepare and execute a LY Rejection Assay (calculating either Papp, Percent Rejection, or both) using Caco-2 monolayers on 12 mm, 0.4 µm transwell inserts and 96-well fluorescent reader plates.

1. Make a solution of 1% DMSO in PBS.
2. Prewarm all reagents before beginning assay:
   - PBS
   - 1% DMSO in PBS
3. Aliquot 1.88 mL of 1% DMSO in PBS to each well of a new receiver plate and place in 37^0C incubator.
4. Remove transwell plate from incubator.
5. Wash each transwell insert 3 times with prewarmed PBS (no DMSO).
   Note: Be sure to wash the monolayers gently in order to preserve monolayer integrity. Wash monolayers until the liquid discarded is no longer pink.
6. Add 600 µL of 60uM LY solution in PBS 1% DMSO to each well of the transwell insert.
7. Remove prepared receiver plate from the incubator.
8. Place transwell insert into receiver plate of step 4.
9. Incubate plate at 37^0C, 5% CO_2 for 1 hour.
10. During the incubation period, make the dilutions for a standard curve.
    - Make LY solutions in PBS 1% DMSO.
    - Make five 1:3 dilutions. Follow the table below to create each solution. Place each solution directly into the black reader plate and gently pipet the solution up and down to mix.

Dilution Number	60µM LY Solution (µL)	PBS 1% DMSO	Concentration of LY Solution (µM)	Absolute Amount LY (nanomoles)
1	200	0	60	12
2	66.67	133.33	20	4
3	22.23	177.78	6.7	1.33
4	7.41	192.59	2.23	0.44
5	2.47	197.53	0.74	0.15

11. Once the incubation period is complete, pipet the entire contents of each receiver plate (basolateral side) and transwell insert (apical side) into respective containers. Record the volumes removed, as they will be used for concentration calculations later.

12. Transfer 200 µL of medium from the receiver plate(s) (basolateral side) into a corresponding well of a solid black plate.

    Note: It is very helpful to make a table of the contents of each well in the plate, as it is easy to lose track.
13. Transfer 50 µL of medium from the transwell insert (apical side) into a corresponding well of the solid black plate. Add 50 µL of PBS 1% DMSO to any well into which apical medium was added.
14. Read plates in an appropriate fluorescent reader (Excitation/Emission wavelength 480 (20) nm/530 (20) nm).
15. In Excel or similar, graph the standard curve in absolute amounts versus RFU value. On the graph, insert a linear line of best fit and display the R^2-value and equation. Using the equation for the line, calculate the absolute amounts of LY for all basolateral and apical medium. Using the absolute amount and the volumes collected in step 11 to calculate the molarity of LY from apical and basolateral sides.

    Note: Remember that the apical medium placed in the reader plate is a 1:2 dilution, so multiply by 2 to get corrected RFU values for wells containing apical medium.
16. Using the calculated final concentration on basolateral side(s) calculate the $P_{app.}$
17. Using the RFU values from apical and basolateral sides, calculate % LY Rejection

    Note: Remember that the apical medium placed in the reader plate is a 1:2 dilution, so multiply by 2 to get corrected RFU values for wells containing apical medium.

Appendix C: Fluorescence Plate Reader Protocol

1. Place the well plate with sample in the fluorescent plate reader. You do not need to leave the lid on the plate for this.
2. Click on the Wallac-1420 icon
3. Click define plate map
4. Find protocol: Wobbe Lab, PW MQP Group
5. Instrument control tab:
    a. Define plate map. Click and highlight and choose empty or measured. This is done by rows.
6. Click next twice, then finish to start reading the plate. The live display tab shows a color legend as the plate is being read. Once the reading is complete, click the latest assay run button. The plate tab gives an excel chart of the numerical readings. To export the file to the desktop, click file → export. Click the shortcut to user data → Weathers. Either create a folder use a premade folder, then save the exported plate data into the folder. The file then exports as an excel file. Because the computer is not connected to a network, save the exported excel to a thumb drive to take it out of the lab.

Appendix D: Solubility of AN, Quercetin, and Rutin in Ethanol

To test the solubility of AN, Q, and R in ethanol, stock solutions of each compound were made in ethanol. An aliquot of each respective stock solution was added to a test tube and diluted with PBS. The diluted samples were then extracted with methylene chloride for analysis with Gas Chromatography/Mass Spectrometry (GC/MS). The exact protocol for this solubility study was as follows.

1. Test tubes containing 200 µg AN, 200 µg Q, and 100 µg R, respectively, were brought up in ethanol to make 1 µg/µL stock solutions.
   - 200 µL ethanol added to each of the AN and Q samples, 100 µL ethanol added to R sample.
2. Aliquots were taken from each stock solution and added to new test tubes. The amount added to each tube was equal to the amount of stock solution needed to make enough dissolved compound in PBS for use on 4 transwells.

Table 1: Contents of solubility study samples

Replicate	Artemisinin Samples	Quercetin Samples	Rutin Samples
1	120 µL AN stock solution 2 mL PBS	24 µL Q stock solution 2 mL PBS	24 µL R stock solution 2 mL PBS
2	120 µL AN stock solution 2 mL PBS	24 µL Q stock solution 2 mL PBS	24 µL R stock solution 2 mL water
3	120 µL AN stock solution	24 µL Q stock solution	24 µL R stock solution

3. Two replicates of each diluted stock solution were made. As a control, undiluted stock solution was also extracted for GC/MS analysis.
4. To extract each diluted sample, 2 mL of methylene chloride was added to each tube. 1 mL of methylene chloride was added to the tubes containing undiluted stock solutions.
5. The methylene chloride from each extraction was transferred to new test tubes using Pasteur pipets.
6. The tubes containing methylene chloride extractions were dried down under nitrogen gas. The dried extractions were then used for GC/MS analysis.

Appendix E: Cell Counting Format and Example

Cell counting is essential for determining the volume of cell suspension to be seeded onto each transwell insert for use in drug transport studies. To count cells, the cells must first be trypsinized from the culture surface, centrifuged, and resuspended in culture medium. Using an aliquot of the resuspended culture, a solution of 50 µL trypan blue and 50 µL cell suspension is created in an Eppendorf tube. This solution is then pipetted onto a hemocytometer. The hemocytometer is then examined under a microscope. Hemocytometers consist of nine 1 mm^2 squares, each of which is divided into smaller squares of 0.2 mm^2 each. To count cells, the entirety of at least one large 1 mm^2 square must be counted. If 100 total cells are not visible in this square, other squares are counted until the number of total cells is at least 100. Each large square must be counted in its entirety, even if the minimum count of 100 is reached before the square has been fully counted.

To determine the number of live cells counted, the number of dead cells, identified by their blue color, is subtracted from the number of total cells counted. If more than one square was used to reach the total number of cells, the number of live cells counted is divided by the number of squares used for the count, giving the number of live cells/mm^2. This number is then converted into live cells/mL using the following formula:

$$Live\ \ cells/mL = \frac{(Live\ cells/mm^2)}{1\ x\ 10^{-4}\ mL} * dilution\ factor\ used\ for\ counting$$

In this formula, 1 x 10^{-4} mL is the volume of one 1 mm^2 square and the dilution factor is 2, as the counting solution was made with 1:1 trypan blue and cell suspension. The concentration of live cells per milliliter is then multiplied by the volume in milliliters of cell suspension available (Freshney, 1994).

Using the calculated cells per milliliter, the number of transwells that can be seeded from the volume of cell suspension available can be calculated by dividing the cells/mL by 300,000, the number of cells needed to seed a 12 mm diameter transwell insert. Conversely, to calculate the volume of cell suspension needed to seed each transwell, the number of cells needed, 300,000, is divided by the calculated cells/mL.

Appendix F: Lucifer Yellow Results & Analysis

The first Lucifer Yellow (LY) assay performed on a single transwell insert was carried out using the Corning Transwell Protocols for 96-well plates. The standard curve results are shown in Table 1 and Figures 1 and 2.

Table 1: Standard curve concentrations and fluorescence readings for Lucifer Yellow

Concentration of LY (µM)	Average Normalized RFU
60.00	222541
20.00	81893
6.67	89761
1.00	18616
0.33	6237
0.11	5588

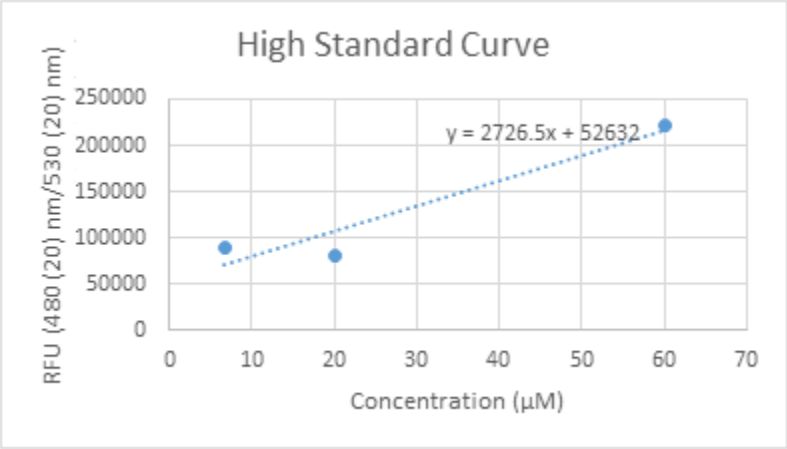

Figure 1: High Lucifer Yellow Standard Curve

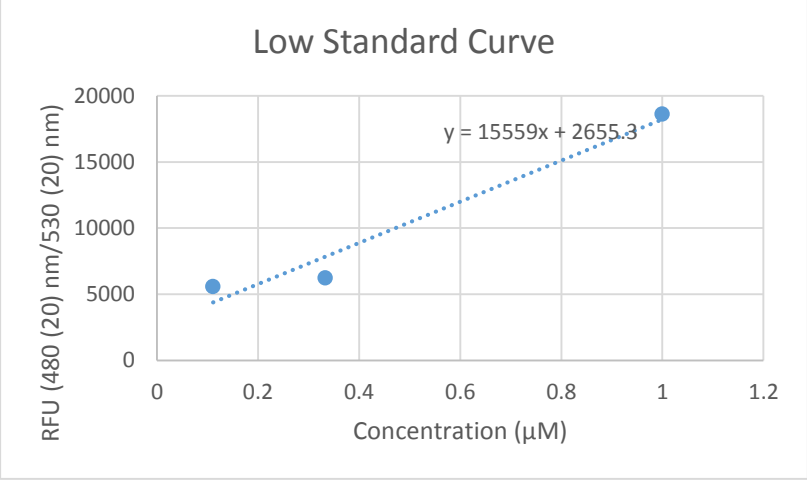

Figure 2: Low Lucifer Yellow Standard Curve

The data points for each concentration did not show a strong linear trend (Figure 1, Figure 2). Table 2 shows the fluorescence readings from the apical and basolateral sides one hour after addition of 60 µM LY in PBS 1% DMSO.

Table 2: Apical and Basolateral Transwell Fluorescence Readings

	Apical RFU	Basolateral RFU
Replicate 1	68518	20478
Replicate 2	69862	21074
Replicate 3	71402	20603
Replicate 4	62322	23393
Average	68026	21387

Using the fluorescence readings shown in Table 2, percent LY rejection was calculated using the formula outlined in the literature review. The resultant % LY rejection value was 68.56%, which did not meet the 80% threshold required for a confluent monolayer in the transwell insert.

Before drug transport studies could be carried out, an LY assay was performed on one of the nine transwell insert to determine whether or not the Caco-2 monolayers were sufficiently confluent for use in transport studies. This LY assay was performed using the LY SOP. Table 3 shows the data used to create the LY standard curve (Figure 3).

Table 3: Amount of LY and Fluorescence Readings for LY Assay 3/17/14

Absolute Amt. of LY (nanomoles)	Absorbance (RFU)
12	419629
4	153281
1.33	53102
0.44	17767
0.15	6864

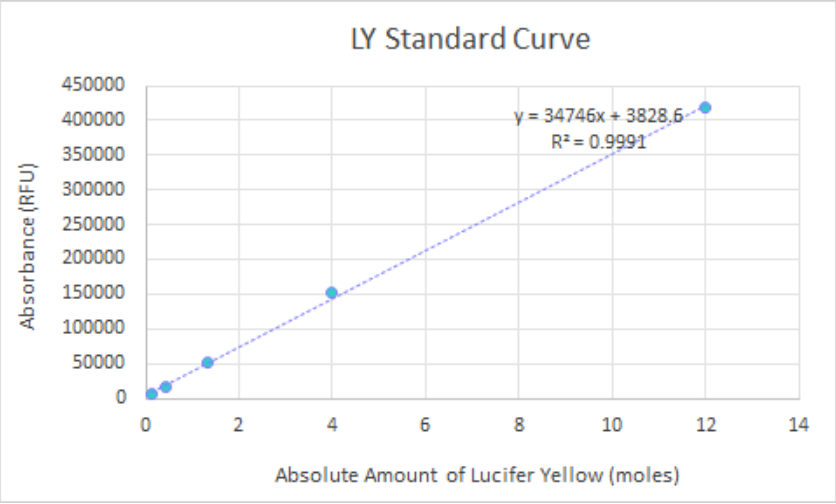

Figure 3: LY Standard Curve for LY Assay 3/17/14

Using this standard curve, the absolute amount of LY on apical and basolateral sides after 60 minute incubation was calculated (Table 4, Table 5).

Table 4: Apical Fluorescence Reading, Amount of LY, and Concentration of LY for LY Assay 3/17/14

Replicate	Absorbance (RFU)	Normalized Absorbance (RFU)	Absolute Amount of LY (nanomoles)
1	64098	126467	3.53
2	48702	95675	2.64
3	60393	119057	3.32
4	64954	128179	4.00
5	61659	121589	3.39
6	63895	126061	3.52

Table 5: Basolateral Fluorescence Reading, Amount of LY, and Concentration of LY for LY Assay 3/17/14

Replicate	Normalized Absorbance (RFU)	Absolute Amount of LY (moles)	Concentration of LY (µM)
1	27685	0.69	3.43
2	29362	0.73	3.67
3	29495	0.74	3.69
4	29054	0.73	3.63
5	30046	0.75	3.77
6	31547	29818	0.75

Using the calculated concentrations, the permeability coefficient (P_{app}) for LY was determined using the formula outlined in the literature review. The calculated permeability coefficient was 2.7 nm/s. The calculated percent LY rejection was 75.53%. Based on these values, the remaining Caco-2 monolayers were deemed sufficiently confluent to proceed with experimentation.

To control for cell damage due to exposure to 5% ethanol during experimentation, one transwell insert was incubated with 5% ethanol in PBS for 60 minutes, after which an LY assay was performed. As before, the amount and concentration of LY on apical and basolateral sides after 60 minutes were calculated (Table 6, Table 7).

Table 6: Apical Fluorescence Reading, Amount of LY, and Concentration of LY for Ethanol Control LY Assay 3/17/14

Replicate	Absorbance (RFU)	Normalized Absorbance (RFU)	Absolute Amount of LY (nanomoles)
1	64229	126729	3.54
2	65946	130163	3.64
3	65591	129453	3.62
4	65560	129391	3.61
5	64858	127987	3.57
6	62898	124067	3.46

Table 7: Basolateral Fluorescence Reading, Amount of LY, and Concentration of LY for LY Assay 3/17/14

Replicate	Absorbance (RFU)	Normalized Absorbance (RFU)	Absolute Amount of LY (nanomoles)
1	22458	20729	0.49
2	22388	20659	0.48
3	22523	20794	0.49
4	22872	21143	0.50
5	22926	21197	0.50
6	22716	20987	0.49

These results yielded a P_{app} of 1.7 nm/s and a percent LY rejection of 83.60%, indicating that the Caco-2 monolayer had not been damaged by ethanol exposure.

Appendix G: GC/MS Raw Data

When all samples from apical to basolateral transport studies were collected and dried with N_2 gas, the samples were analyzed using Gas Chromatography/Mass Spectrometry (GC/MS) (Table 1, Table 2, Table 3).

Table 1: AN Transport

Vial	µg AN/vial	Concentration of AN (µg/mL) in Transport Media
AN1 0 Apical	19.99	39.98
AN2 0 Apical	20.78	41.57
AN3 0 Apical	17.09	34.18
AN1 15 Basolateral	0.33	0.22
AN2 15 Basolateral	0.59	0.39
AN3 15 Basolateral	0.94	0.62
AN1 30 Basolateral	0.15	0.10
AN2 30 Basolateral	0.12	0.08
AN3 30 Basolateral	0.14	0.09
AN1 45 Basolateral	0.14	0.09
AN2 45 Basolateral	0.08	0.05
AN3 45 Basolateral	0	0
AN1 60 Basolateral	0.32	0.21
AN2 60 Basolateral	0.18	0.12
AN3 60 Basolateral	0.25	0.17
AN1 60 Apical	2.32	4.63
AN2 60 Apical	2.73	5.46
AN3 60 Apical	3.28	6.55

Table 2: AN + Q Transport

Vial	µg AN/vial	Concentration of AN (µg/mL) in Transport Media
AN + Q1 0 Apical	13.91	27.82
AN + Q2 0 Apical	18.82	37.64
AN + Q1 15 Basolateral	0.60	0.40
AN + Q2 15 Basolateral	0.36	0.24
AN + Q1 30 Basolateral	0.42	0.28
AN + Q2 30 Basolateral	0.32	0.22
AN + Q1 45 Basolateral	0.21	0.14
AN + Q2 45 Basolateral	0.41	0.27
AN + Q1 60 Basolateral	0.45	0.30
AN + Q2 60 Basolateral	0.20	0.14
AN + Q1 60 Apical	4.15	8.29
AN + Q2 60 Apical	4.04	8.08

Table 3: AN + R Transport

Vial	µg AN/vial	Concentration of AN (µg/mL) in Transport Media
AN + R1 0 Apical	16.97	33.94
AN + R2 0 Apical	15.85	31.69
AN + R1 15 Basolateral	0.50	0.33
AN + R2 15 Basolateral	0.57	0.38
AN + R1 30 Basolateral	0.71	0.47
AN + R2 30 Basolateral	0.16	0.11
AN + R1 45 Basolateral	0.12	0.08
AN + R2 45 Basolateral	0.11	0.08
AN + R1 60 Basolateral	0.50	0.33
AN + R2 60 Basolateral	0.69	0.46
AN + R1 60 Apical	9.15	18.30
AN + R2 60 Apical	2.44	4.89

Table 4: Q and R Data

Experimental Treatment	Sampling Time	µg/vial (Q equivalents)
AN + Q	0 Apical	4.80
	60 Apical	2.24
	60 Basolateral	0.48
AN + R	0 Apical	0.41
	60 Apical	12.83
	60 Basolateral	1.15